Phytoplasma SAP11 effector destabilization of TCP transcription factors differentially impact development and defence of Arabidopsis versus maize

Short title: SAP11 targeting of TCPs impacts maize architecture but not defence.

Pascal Pecher[1¶], Gabriele Moro[1¶], Maria Cristina Canale[1,2,#a], Sylvain Capdevielle[1], Archana Singh[1,#b], Allyson MacLean[1,#c], Akiko Sugio[1,#d], Chih-Horng Kuo[3], Joao R. S. Lopes[2] and Saskia A. Hogenhout[1]

[1]John Innes Centre, Department of Crop Genetics, Norwich Research Park, Norwich NR4 7UH, UK

[2]Luiz de Queiroz College of Agriculture, Department of Entomology and Acarology, University of São Paulo, Piracicaba 13418-900, Brazil

[3]Academia Sinica, Institute of Plant and Microbial Biology, Taipei, Taiwan.

[#a] Agricultural Research Company of Santa Catarina State (Epagri), Chapeco 89809-450, Brazil

[#b] Earlham Institute, Norwich Research Park, Norwich NR4 7UZ, UK.

[#c] Department of Biology, University of Ottawa, Ottawa, ON, K1N 6N5, Canada.

[#d] INRA, UMR Institut de Génétique, Environnement et Protection des Plantes (IGEPP) Domaine de la Motte, 35653 Le Rheu cedex - France

*Corresponding author:

Email: *saskia.hogenhout@jic.ac.uk*

¶These authors contributed equally to this work

Abstract

Phytoplasmas are insect-transmitted bacterial pathogens that colonize a wide range of plant species, including vegetable and cereal crops, and herbaceous and woody ornamentals. Phytoplasma-infected plants often show dramatic symptoms, including proliferation of shoots (witch's brooms), changes in leaf shapes and production of green sterile flowers (phyllody). Aster Yellows phytoplasma Witches' Broom (AY-WB) infects dicots and its effector, secreted AYWB protein 11 (SAP11), was shown to be responsible for the induction of shoot proliferation and leaf shape changes of plants. SAP11 acts by destabilizing TEOSINTE BRANCHED 1-CYCLOIDEA-PROLIFERATING CELL FACTOR (TCP) transcription factors, particularly the class II TCPs of the CYCLOIDEA/TEOSINTE BRANCHED 1 (CYC/TB1) and CINCINNATA (CIN)-TCP clades. SAP11 homologs are also present in phytoplasmas that cause economic yield losses in monocot crops, such as maize, wheat and coconut. Here we show that a SAP11 homolog of Maize Bushy Stunt Phytoplasma (MBSP), which has a range primarily restricted to maize, destabilizes only TB1/CYC TCPs. $SAP11_{MBSP}$ and $SAP11_{AYWB}$ both induce axillary branching and $SAP11_{AYWB}$ also alters leaf development of *Arabidopsis thaliana* and maize. However, only in maize, $SAP11_{MBSP}$ prevents female inflorescence development, phenocopying maize *tb1* lines, whereas $SAP11_{AYWB}$ prevents male inflorescence development and induces feminization of tassels. $SAP11_{AYWB}$ promotes fecundity of the AY-WB leafhopper vector on *A. thaliana* and modulates the expression of *A. thaliana* leaf defence response genes that are induced by this leafhopper, in contrast to $SAP11_{MBSP}$. Neither of the SAP11 effectors promote fecundity of AY-WB and MBSP leafhopper vectors on maize. These data provide evidence that class II TCPs have overlapping but also distinct roles in regulating development and defence in a dicot and a monocot plant species that is likely to shape SAP11 effector evolution depending on the phytoplasma host range.

Keywords: Insect vector; Phytoplasma; Plant architecture; Plant defence response; Plant development; Plant-insect interactions; SAP11 effectors; TCP transcription factors.

Author summary

Phytoplasmas are parasites of a wide range of plant species and are transmitted by sap-feeding insects, such as leafhoppers. Phytoplasma-infected plants are often easily recognized because of their dramatic symptoms, including shoot proliferations (witch's brooms) and altered leaf shapes, leading to severe economic losses of crops, ornamentals and trees worldwide. We previously found that the virulence protein SAP11 of aster yellows witches' broom phytoplasma (AY-WB) interferes with a specific group of plant transcription factors, named TCPs, leading to witches' brooms and leaf shape changes of the model plant *Arabidopsis thaliana*. SAP11 has been characterized in a number of other phytoplasmas. However, it is not known how phytoplasmas and their SAP11 proteins modulate processes in crops, including cereals such as maize. We identified a SAP11 homolog in Maize bushy stunt phytoplasma (MBSP), a pathogen that can cause severe yield losses of maize. We found that SAP11 interactions with TCPs are conserved between maize and Arabidopsis, and that MBSP SAP11 interferes with less TCPs compared to AY-WB SAP11. This work provides new insights into how phytoplasmas change maize architecture and corn production. Moreover, we found that TCPs regulate leaf defence responses to phytoplasma leafhopper vectors in Arabidopsis, but not in maize.

Introduction

Phytoplasmas ("*Candidatus* (*Ca.*) Phytoplasma") are economically important plant pathogens that infect a broad range of plant species. The more than 1000 phytoplasmas described so far comprise three distinct clades within a monophyletic group of the class Mollicutes that are characterized by the lack of a bacterial cell wall and small genomes (580 kb to 2200 kb) [1-3]. These fastidious pathogens are restricted to the phloem sieve cells of the plant vasculature and depend on phloem-sap-feeding insect vectors, including leafhoppers, planthoppers and psyllids, for transmission and spread in nature [4]. Many phytoplasmas induce dramatic changes in plant architecture such as increased axillary branching (often referred to as witches' broom), formation of leaf-like flowers (phyllody), the production of green floral organs such as petals and stamens (virescence), changes of leaf shape, and premature bolting [5-10].

Phytoplasmas change plant architecture via the secretion of proteinaceous effectors that interact with and destabilize plant transcription factors with fundamental roles in regulating plant development. Effectors of Aster yellows phytoplasma strain Witches Broom (AY-WB; "*Ca*. Phytoplasma asteris") are particularly well characterized. AY-WB and its predominant leafhopper vector *Macrosteles quadrilineatus* have broad host ranges that mostly include dicots, including *Arabidopsis thaliana* [6]. SAP11 destabilizes Arabidopsis TEOSINTE BRANCHED1-CYCLOIDEA-PROLIFERATING CELL FACTOR (TCP) transcription factors, and specifically class II TCPs, leading to the induction of axillary branching and changes in leaf shape of this plant [8,11], and SAP54 degrades Arabidopsis MADS-box transcription factors leading to changes in flower development that resemble phyllody and virescence symptoms [9,12]. Moreover, both effectors modulate plant defence responses leading to increased colonization of *M. quadrilineatus* on *A. thaliana* [8,9,13]. For $SAP11_{AYWB}$ this involves the inhibition of jasmonate (JA) synthesis [8]. SAP11 and SAP54

homologs of other phytoplasmas also target TCPs and MADS, respectively, leading to corresponding changes in plant development and architecture [10,14-16]. The majority of phytoplasma effector genes lie within composite-transposon-like pathogenicity islands named potential mobile units (PMUs) that are prone to recombination and horizontal gene transfer [17-20].

Maize bushy stunt phytoplasma (MBSP) belongs to the Aster yellows (AY) group (16SrI) "*Ca*. P. asteris" [21] and is the only known member of this group to be largely restricted to maize (*Z. mays* L.), whereas the majority, including AY-WB, are transmitted by polyphagous insects and infect dicotyledonous plants [13,22]. MBSP is transmitted by the maize-specialist insects *Dalbulus maidis* and *D. elimatus*; both MBSP and insect vectors are thought to have co-evolved with maize since its domestication from teosinte [23]. Symptoms of MBSP-infected maize plants include the formation of long lateral branches, decline in ear development and emergence of leaves that are often twisted with ripped edges and that display chlorosis and reddening [13]. We previously identified a SAP11 homolog in the MBSP genome [22] and $SAP11_{MBSP}$ is identical in sequence among multiple MBSP isolates collected from Mexico and Brazil [13]. $SAP11_{AYWB}$ and $SAP11_{MBSP}$ lie on microsyntenic regions within the phytoplasma genomes, indicating that these effectors are likely to have common ancestry [13]. However, *D. maidis* does not produce more progeny on MBSP-infected plants that show advanced disease symptoms; the insects prefer infected plants that are non-symptomatic [24]. In this study we wished to compare the roles of $SAP11_{AYWB}$ and $SAP11_{MBSP}$ in symptom induction and plant defence to insect vectors of *A. thaliana* and maize.

TCP transcription factors comprise an ancient plant-specific family [25] that are distinguished from other transcription factors by a conserved ± 60 amino acid TCP domain [26]. The TCP domain consists of a helix-loop-helix region that form TCP homo or

heterodimers and a basic region that mediates interactions of TCP dimers with DNA motifs [27] and is required for SAP11 binding to TCPs [11]. TCP transcription factors are grouped into three clades based on TCP domain sequences: (i) class I PROLIFERATING CELL FACTOR-type TCPs (PCF clade); (ii) class II CINCINNATA-type TCPs (CIN clade); and (iii) class II CYCLOIDEA/TEOSINTE BRANCHED 1-type TCPs (CYC/TB1-clade) [28]. The latter is also known as the glutamic acid-cysteine-glutamic acid (ECE) clade [29]. PCFs promote cell proliferation, whereas CIN clade TCPs promote leaf and petal cell maturation and differentiation and have antagonistic roles to PCFs [30-33]. The ECE clade includes maize TEOSINTE BRANCHED 1 (TB1) and TB1 homologs of *A. thaliana* BRANCHED 1 (BRC1) and BRC2, that repress the development of axillary branches in plants [34-37], and CYCLOIDEA (CYC) that control flower symmetry [38]. TB1 and genes in the TB1 network have been targeted for selection during maize domestication from a teosinte ancestor [39,40].

Here we show that $SAP11_{AYWB}$ and $SAP11_{MBSP}$ have overlapping but distinct specificities for destabilizing class II TCP transcription factors. The SAP11 effectors induce unique phenotypes in Arabidopsis and maize that indicate divergent roles of class II TCP transcription factors in regulating development and defence in the two plant species. We argue that $SAP11_{MBSP}$ evolution may be constrained due to the specific functionalities of class II TCPs in maize.

Results

Phytoplasma $SAP11_{AYWB}$ binds and destabilizes both Arabidopsis CIN and CYC/TB1 TCPs and $SAP11_{MBSP}$ only CYC/TB1 TCPs

$SAP11_{AYWB}$ and $SAP11_{MBSP}$ interaction specificities for Arabidopsis TCPs (AtTCPs) were investigated via yeast two-hybrid (Y2H) assays and protein destabilization assays in

A. thaliana mesophyll protoplasts. In the protoplast experiments, $SAP11_{AYWB}$ destabilized the majority of AtCIN-TCPs and none of the class I AtTCPs (Fig. 1A), confirming previous results [8]. In addition, $SAP11_{AYWB}$ also destabilized CYC/TB1-TCPs BRC1 and BRC2 but not the five Arabidopsis class I TCPs (Fig. 1A). In contrast, $SAP11_{MBSP}$ destabilized the CYC/TB1 TCPs BRC1 and BRC2, whereas 7 out of 8 class II AtCIN-TCPs and all tested class I AtTCPs remained stable (Fig. 1A). The Y2H assays showed that $SAP11_{AYWB}$ interacts with Arabidopsis CIN-TCPs (Fig. 1B), confirming previous data [8,11], whereas $SAP11_{MBSP}$ did not (Fig. 1B). However, both $SAP11_{AYWB}$ and $SAP11_{MBSP}$ interacted with CYC/TB1 BRC1 and BRC2 (Fig. 1B). Therefore, $SAP11_{MBSP}$ binds and destabilizes a narrower set of class II TCPs compared to $SAP11_{AYWB}$.

To investigate which region of TCP domain determine SAP11 binding specificity, chimeras of the basic region and helix loop helix regions of the TCP domains of CIN-TCP AtTCP2 and CYC/TB1-TCP BRC1 (AtTCP18) were constructed (Fig. 2) and tested for interactions with the two SAP11 proteins in yeast two-hybrid analyses. $SAP11_{AYWB}$ and $SAP11_{MBSP}$ interacted with the TCP domains of AtTCP2 and BRC1 (Fig. 2B), as observed for full length TCPs (Fig. 1B), confirming that the TCP domain itself is sufficient for SAP11 interaction and specificity. Furthermore, $SAP11_{AYWB}$ interacted with all AtTCP2-BRC1 chimeras used in the assay (Fig. 2), whereas $SAP11_{MBSP}$ interacted with chimeras containing BRC1 helix-loop-helix and AtTCP2 basic regions, but not with those composed of AtTCP2 helix-loop-helix and BRC1 basic region or with mixed helix, loop and helix sequences (Fig. 2). Therefore, the entire helix-loop-helix region of the TCP domain is required for the specific binding of $SAP11_{MBSP}$ to CYC/TB1 TCPs.

A. thaliana plants stably expressing $SAP11_{MBSP}$ and $SAP11_{AYWB}$ phenocopy *brc1 brc2* mutant or CIN-TCP knock down lines

To investigate if the SAP11 binding specificity to TCPs aligns with *in planta* interactions, phenotypes of *A. thaliana* Col-0 stable transgenic lines that produce $SAP11_{AYWB}$ and $SAP11_{MBSP}$ under control of the 35S promoter (Fig. 1C) were compared to those of the *A. thaliana brc1-2 brc2-1* double mutant, hereafter referred to as the *brc1 brc2* mutant, which is a *null* mutant for both CYC/TB1-TCPs BRC1 and BRC2 [34] and the *35S::miR319a x 35S::miR3TCP* line in which CIN-TCPs are knocked down [30]. Whereas the crinkled leaves of *35S::SAP11*$_{AYWB}$ lines phenocopied those of *35S::miR319a x 35S::miR3TCP* (Fig. 1D) [8], leaves of *35S::SAP11*$_{MBSP}$ lines were not crinkled and more similar to WT Col-0 leaves (Fig. 1D). Rosette diameters of the *35S::SAP11*$_{AYWB}$ and *35S::miR319a x 35S::miR3TCP* lines were smaller than WT Col-0 plants, unlike the rosettes of *35S::SAP11*$_{MBSP}$ and *A. thaliana brc1 brc2* mutant lines that looked similar to those of WT plants (Fig. 1F). Both *35S::SAP11*$_{AYWB}$ and *35S::SAP11*$_{MBSP}$ lines produced significantly more primary rosette-leaf branches (RI) [34] than WT plants. With exception of the *35S::SAP11*$_{MBSP}$ line 3 that had a lower number of RIs, the production of RI was similar to the *A. thaliana brc1 brc2* mutant. In contrast, *35S::miR319a x 35S::miR3TCP* plants produced a reduced number of RI compared to WT Col-0 (Figs. 1E and 1G, S1E Fig.). Therefore, *35S::SAP11*$_{MBSP}$ lines phenocopied the *A. thaliana brc1 brc2* mutant and the *35S::SAP11*$_{AYWB}$ lines both the *A. thaliana brc1 brc2* and *35S::miR319a x 35S::miR3TCP* mutant lines, indicating that $SAP11_{AYWB}$ destabilizes Arabidopsis CIN and CYC/TB1 TCPs and $SAP11_{MBSP}$ only the CYC/TB1-TCPs BRC1 and BRC2, in agreement with the results of protoplast-based destabilization and Y2H binding assays.

Beyond phenotypes described above, we found that the *35S::miR319a x 35S::miR3TCP* and *35S::SAP11*$_{AYWB}$ lines produced less rosette leaves compared to WT plants, unlike the *A. thaliana brc1 brc2* and *35S::SAP11*$_{MBSP}$ lines (S1A Fig.). Bolting time, plant height and numbers of primary cauline-leaf branches (CI) [34] were variable among the *35S::SAP11*$_{AYWB}$

and *35S::SAP11*$_{MBSP}$ lines (S1B-S1E Figs.). Roots of *35S::miR319a x 35S::miR3TCP* and *35S::SAP11*$_{AYWB}$ lines were consistently shorter compared to WT plants as described by Lu *et al*. [41]. In contrast, the root length of *A. thaliana brc1 brc2* and *35S::SAP11*$_{MBSP}$ lines did not show obvious differences compared to those of WT plants (S2 Fig.).

SAP11$_{AYWB}$ impairs *A. thaliana* defence responses to *M. quadrilineatus* in contrast to SAP11$_{MBSP}$

We previously showed that the AY-WB insect vector *M. quadrilineatus* produces 20-30% more progeny on *35S::SAP11*$_{AYWB}$ *A. thaliana* [8]. By repeating this experiment and including *35S::SAP11*$_{MBSP}$ *A. thaliana*, we confirmed the previous result for *35S::SAP11*$_{AYWB}$ *A. thaliana* but not for *35S::SAP11*$_{MBSP}$ *A. thaliana* (Fig. 3A). Therefore, SAP11$_{AYWB}$ appears to modulate plant defences in response to *M. quadrilineatus*, whereas SAP11$_{MBSP}$ does not. To test this further, the transcriptomes of wild type, *35S::SAP11*$_{AYWB}$ and *35S::SAP11*$_{MBSP}$ *A. thaliana* with and without exposure to *M. quadrilineatus* were compared via RNA-seq (S1 Table, GEO accession GSE118427). PCA showed that, in samples exposed to *M. quadrilineatus*, *35S::SAP11*$_{MBSP}$ and WT Col-0 group together, whereas the *35S::SAP11*$_{AYWB}$ samples form a separate group (Fig. 3B). Therefore, SAP11$_{AYWB}$ has a measurable impact on the transcriptome of *A. thaliana*, unlike SAP11$_{MBSP}$.

Analyses of differentially expressed genes (DEGs) of Col-0 and transgenic plants exposed to *M. quadrilineatus* identified 96 DEGs for *35S::SAP11*$_{AYWB}$ versus Col-0 and only one DEG for *35S::SAP11*$_{MBSP}$ versus Col-0 (Figs. 3C and 3D). Hierarchical cluster of the DEGs expression levels was in agreement with the PCA results demonstrating that the *M. quadrilineatus*-exposed 35S::SAP11$_{AYWB}$ treatments cluster separately from those of Col-0 and 35S::SAP11$_{MBSP}$ (Fig. 3E, S2 Table). Moreover, *M. quadrilineatus*-exposed 35S::SAP11$_{AYWB}$ treatments cluster together with non-exposed samples. Of the 96 DEGs 30

have a role in regulating plant defence responses, including hormone and secondary metabolism, such as Myb, AP2/EREBP and bZIP transcription factors, receptor kinases, cytochrome P450 enzymes, proteases, oxidases and transferases (highlighted in yellow, S3 Table). The 96 genes also included 11 natural anti-sense genes and at least 30 genes with unknown functions. Taken together, these data indicate that defence responses to *M. quadrilineatus* are suppressed in 35S::SAP11$_{AYWB}$ plants.

Identification of maize TCP transcription factors

To investigate SAP11 interactions with maize TCPs we first identified maize TCP sequences. The CDS of 44 *Z. mays* (Zm) TCPs available on maize TFome collection [42] were extracted from the Grass Regulatory Information Server (GRASSIUS) (http://grassius.org/grasstfdb.html) [43]. We identified two class II CYC/TB1-TCPs, including TB1 and ZmTCP18, 10 class II CIN-TCPs and 17 class I PCF-like TCPs. The ZmTCPs were assigned to groups based on characteristic TCP domain amino acids conserved in each of the groups, highlighted in yellow, red and green (Fig. 4) [28]. In contrast to *A. thaliana*, maize appears to have an additional group of class II TCPs that share amino acids conserved in the TCP domains of both CIN and TB1/CYC TCPs (Fig. 4). One of these is BRANCHED ANGLE DEFECTIVE1 (BAD1), which is expressed in the pulvinus to regulate branch angle emergence of inflorescences, particularly the tassel [44]. BAD1 was placed in a subclade of CYC-TB1 TCPs named as TCP CII. Hence, we assigned all members in this additional group to TCP CII. TCPs similar to TCP CII appear to be absent in the monocots rice (*O. sativa*) and sorghum (*S. bicolor*) (S3 and S4 Figs., S4 Table). Seven CIN-TCPs of maize, rice and sorghum are potentially regulated by miR319a (Fig. 4, S3-S5 Figs). While this study was ongoing, Chai *et al.* [45] reported the expression characteristics of 29 maize TCPs. To promote consistency, we adopted their nomenclature for these TCPs as

ZmTCP01 to ZmTCP29, and continued the numbering of the additional 15 maize TCP genes extracted from GRASSIUS as ZmTCP30 to ZmTCP45 (Fig. 4, S4 Table).

Phytoplasma SAP11 homologs interact with and destabilize maize class II TCPs

Y2H assays revealed that $SAP11_{MBSP}$ interacts with the CYC/TB1-TCPs ZmTCP02 (TB1) and ZmTCP18, but not with ZmTCP members of the CIN and CII subgroups (Fig. 5A). In contrast, $SAP11_{AYWB}$ interacted also with CIN and CII ZmTCPs (Fig. 5A). GFP-$SAP11_{MBSP}$ and GFP-$SAP11_{AYWB}$ destabilized HA-tagged ZmTCP02 (TB1) and ZmTCP18 in maize protoplasts in contrast to GFP controls (Fig. 5B), indicating that the SAP11 homologs also destabilize maize TCPs in maize cells.

Stable *$SAP11_{MBSP}$* and *$SAP11_{AYWB}$* transgenic maize plants lack female and male sex organs, respectively

$SAP11_{AYWB}$ and *$SAP11_{MBSP}$* were cloned as N-terminal 3XFLAG tag fusions downstream of the maize Ubiquitin promoter, and transformed into HiIIAXHiIIB hybrid *Z. mays*. *Ubi::FLAG-$SAP11_{MBSP}$* primary transformants (T_0) were female sterile, but produced pollen, which were used for fertilizing flowers of a wild type HiIIA plant. In contrast, *Ubi::FLAG-$SAP11_{AYWB}$* primary transformants were male sterile, but produced flowers, which were successfully fertilized with pollen from a HiIIA plant. The T_1 progenies of both crosses had similar production of SAP11 proteins (Fig. 5C) and were further phenotyped.

Unlike WT HiIIA, *Ubi::FLAG-$SAP11_{MBSP}$* T_1 plants produced multiple tillers arising from the base of the main culm (Figs. 5D (a, c) and 6). Both main culm and tillers produced apical male inflorescences with tassels that carried anthers with pollen (Figs. 5D (j, l, insets 7, 10, 11) and 6). These pollen were fertile, as they were used to pollinate HiIIA female inflorescence for seed reproduction. At the upper nodes of the main culm where in WT plants

short primary lateral branches with apical ears would develop from the leaf sheath (Figs 5D (g) and 6), long primary lateral branches emerged that also had apical tassels (Figs 5D (i, inset 3) and 6). Hence, *Ubi::FLAG-SAP11*$_{MBSP}$ plants were female sterile. These phenotypes of *Ubi::FLAG-SAP11*$_{MBSP}$ plants are similar to those of the *Z. mays tb1* mutant (Fig. 6) [39,46]. Essentially, *Ubi::FLAG-SAP11*$_{MBSP}$ and *Z. mays tb1* mutant lines resemble teosinte, though the latter produces small ears located at multiple lateral positions of the primary lateral branches (Fig. 6) [47]. Therefore, *Ubi::FLAG-SAP11*$_{MBSP}$ plants phenocopy the maize *tb1* mutant, in agreement with results of yeast two-hybrid and protoplast destabilization assays showing that SAP11$_{MBSP}$ destabilizes CYC/TB1 TCPs.

Ubi::FLAG-SAP11$_{AYWB}$ T_1 plants also produced more tillers from the base of the main culm, but were shorter than WT HiIIA and *Ubi::FLAG-SAP11*$_{MBSP}$ (Fig. 5D (a, b, c)). The majority of leaves of *Ubi::FLAG-SAP11*$_{AYWB}$ plants had curly edges, unlike *Ubi::FLAG-SAP11*$_{MBSP}$ and HiIIA plants (Fig. 5D (d, e, f, h, inset 2)). *Ubi::FLAG-SAP11*$_{AYWB}$ plants produced red-coloured silks emerging directly from the leaf sheath without prior ear formation (Figs. 5D (h, inset 2) and 6). Upon pollination of the red-coloured silks, ears with reduced husk leaves and exposed corn emerged (Fig. 5E (o)). As well, the tip of the main culm and tillers carried tassel-like structures with female flowers and emerging silks (Figs. 5D (k, insets 8, 9) and 6). Pollination of these silks with HIIA pollen induced the formation of a few corns (Fig. 5E (m,n)). Thus, *SAP11*$_{AYWB}$ induces tassel feminization and interferes with leaf development, including the modified leaves that generate the husk of the ear.

SAP11$_{AYWB}$ or SAP11$_{MBSP}$ do not alter maize susceptibility to *M. quadrilineatus* and *D. maidis*

We investigated if SAP11$_{AYWB}$ and SAP11$_{MBSP}$ modulate maize processes in response to the AY-WB and MBSP insect vectors *M. quadrilineatus* and *D. maidis*, respectively. We

300 did not observe any differences in fecundity of both insect vectors on HiIIA, *Ubi::FLAG-*
301 *SAP11$_{AYWB}$* and *Ubi::FLAG-SAP11$_{MBSP}$* plants (Fig. 7A and B). PCA of RNA-seq data from
302 WT and transgenic maize plants indicate that SAP11$_{AYWB}$ and SAP11$_{MBSP}$ modulate maize
303 transcriptomes with SAP11$_{AYWB}$ having a larger effect than SAP11$_{MBSP}$ (Fig. 7C and D, S5
304 and S6 Tables, GEO: GSE118427), in agreement with morphological data of the maize lines
305 (Figs. 5 and 6). However, *M. quadrilineatus*-exposed HiIIA *Ubi::FLAG-SAP11$_{AYWB}$* and
306 *Ubi::FLAG-SAP11$_{MBSP}$* maize clustered together and separately from non-exposed maize in
307 PCA (Fig. 7C). *D. maidis* exposed maize samples grouped with the non-exposed ones (Fig.
308 7D), suggesting that the SAP11 homologs do not have obvious effects on transcriptome
309 responses of maize to the insects. Moreover, *M. quadrilineatus* has a larger impact and
310 *D. maidis* a minor impact on maize gene expression (Fig. 7C and D). Together, these data
311 indicate that SAP11$_{AYWB}$ and SAP11$_{MBSP}$ do not alter maize susceptibility to
312 *M. quadrilineatus* and *D. maidis*.
313

314 ## Discussion

315 We found that SAP11$_{AYWB}$ and SAP11$_{MBSP}$ have overlapping, but distinct, binding
316 specificities for class II TCP transcription factors. The two effectors bind to the TCP domain
317 helix-loop-helix region. This region is required for TCP-TCP dimerization and configuration
318 of the TCP domain beta sheets of both TCP transcription factors in a way that allows binding
319 of the beta sheets to promoters [27]. We also found that SAP11-TCP binding specificities are
320 correlated with the ability of the SAP11 homologs to destabilize these TCPs in leaves [8] and
321 protoplasts (this study) and the induction of specific phenotypes in plants [8, this study].
322 Whereas it remains to be resolved how SAP11 destabilizes TCPs, it is clear that SAP11 is
323 highly effective at destabilizing TCPs in plants as evidenced by the specific SAP11-induced

changes in *A. thaliana* and maize architectures that phenocopy TCP mutants and knock-down lines of these plants.

TCP domains of each TCP (sub)class have characteristic amino acid sequences that have remained conserved after the divergence of monocots and eudicots [48]. We found that SAP11 binding specificity is determined by TCP (sub)class rather than plant species, as $SAP11_{MBSP}$ specifically interacts with class II CYC/TB1-TCPs of both *A. thaliana* and maize, and not class II CIN-TCP and class I TCPs of these divergent plant species. Similarly, $SAP11_{AYWB}$ interacts with all class II TCPs and not the class I TCPs of *A. thaliana* and maize. Therefore, $SAP11_{AYWB}$ and $SAP11_{MBSP}$ binding specificity is likely to involve amino acids within the helix-loop-helix region of the TCP domain that are characteristic for each TCP (sub)class and are conserved among plants species, including dicots and monocots.

We found that $SAP11_{MBSP}$ specifically interacts with and destabilizes TCPs of the TB1 clade, including *A. thaliana* BRC1 and BRC2 and maize TCP02 and TCP18. These binding specificities are supported by plant phenotypes; *A. thaliana 35S::SAP11*$_{MBSP}$ and maize *Ubi::FLAG-SAP11*$_{MBSP}$ lines phenocopy *A. thaliana brc1 brc2* lines and maize *tb1* lines, respectively. The *A. thaliana 35S::SAP11*$_{MBSP}$ lines show stem proliferations, in agreement with *A. thaliana* BRC1 and BRC2 and maize TB1 (ZmTCP02) being suppressors of axillary bud growth [37,49-51]. We also show that *A. thaliana 35S::SAP11*$_{MBSP}$ and *brc1 brc2* lines produce fully fertile flowers, whereas maize *Ubi::FLAG-SAP11*$_{MBSP}$ plants produced only male tassels and no female inflorescences like maize tb1 plants [39,46]. This is in agreement with BRC1 not directly affecting *A. thaliana* flower architecture [52,53], and maize TB1 being a direct positive regulator of MADS-box transcription factors that control maize female inflorescence architecture [40]. Interestingly, many phytoplasmas have SAP54 effectors, which degrade MADS-box transcription factors leading to the formation of leaf-like sterile flowers [9,10,54,55] whereas no effector gene with sequence similarity to SAP54 was

identified in MBSP [56]. It is possible that the maize-specialist phytoplasma strain does not require an additional effector (such as SAP54) to modulate floral development of its host, as $SAP11_{MBSP}$ indirectly targets flowering via TB1.

Whereas $SAP11_{MBSP}$ interacts and destabilizes TB1 TCPs, $SAP11_{AYWB}$ interacts with all class II TCPs of *A. thaliana* and maize, in agreement with *A. thaliana 35S::SAP11$_{AYWB}$* lines phenocopying both *A. thaliana brc1 brc2* and *A. thaliana 35S::miR319a x 35S::miR3TCP* lines. Information about the role of TCPs in maize development are limited, potentially due to redundant functions of TCPs belonging to the same subgroup and the challenges of obtaining multiple knockdown lines. Therefore, at this time we do not know if *maize Ubi::FLAG-SAP11$_{AYWB}$* lines phenocopy maize mutant lines for all CIN and CII TCPs. Nonetheless the leaf crinkling phenotypes of *Ubi::FLAG-SAP11$_{AYWB}$* maize plants are in agreement with what is known about the functions of CIN TCPs in Arabidopsis where CIN TCPs play a role in leaf development [8,32,57]. The CII subgroup member BAD1 regulates branch angle emergence of the maize tassel [44] indicating that CII TCPs regulate male inflorescence development in maize. Our finding that *Ubi::FLAG-SAP11$_{AYWB}$* maize plants solely producing female inflorescences and no tassels expands the current knowledge about maize CII and CIN-TCPs to a potential role in plant sex determination. We cannot fully exclude the possibility that $SAP11_{AYWB}$ destabilizes other proteins in maize, though we think this is unlikely given our finding that SAP11-TCP interactions are specific involving conserved TCP helix-loop-helix sequences and that $SAP11_{AYWB}$ induces changes in *A. thaliana* development that are entirely consistent with destabilization of class II TCPs in this plant. Therefore, phenotypes seen of *Ubi::FLAG-SAP11$_{AYWB}$* maize plants are likely caused by $SAP11_{AYWB}$-mediated destabilization of all maize class II TCPs, indicating a direct role of these TCPs in the development of maize male and female inflorescence architectures.

We previously demonstrated that 35S::SAP11$_{AYWB}$ *A. thaliana* plants are affected in jasmonate production and *LOX2* expression upon wounding and that the AY-WB insect vectors produce more progeny on *LOX2*-silenced plants [8]. A number of TCPs have roles in plant JA production regulation [31,58-63]. Here, we show a clear role of SAP11$_{AYWB}$ suppression of plant defence response genes to *M. quadrilineatus*, including those involved in phytohormone responses. These genes were not differentially regulated in SAP11$_{MBSP}$ plants response to *M. quadrilineatus*, indicating that destabilization of CIN-TCPs alone or in combination with Arabidopsis BRC1 and BRC2 alters plant defence responses to *M. quadrilineatus*. SAP11$_{AYWB}$ does not promote *M. quadrilineatus* and *D. maidis* fecundity on maize suggesting that maize class II TCPs do not play a major role in regulating defence responses of maize leaves. Therefore, class II TCPs appear to regulate plant defence responses in leaves of Arabidopsis but not in maize.

MBSP and the insect vectors *D. maids* and *D. elimatus* are thought to have co-evolved with maize since its domestication from teosinte [23]. We previously sequenced the genomes of MBSP isolates from geographically distant locations and found single nucleotide polymorphisms (SNPs) throughout the genomes of these isolates but that SAP11$_{MBSP}$ remained conserved [56]. The effector may be subject to purifying selection because the destabilization of maize TB1 TCPs and subsequent induction of axillary branching and inhibition of female flower production promote MBSP fitness in maize in a manner that is so far unknown. As well, SAP11$_{MBSP}$ evolution may be constrained by possibly negative effects of maize CIN and ECE TCP destabilization on MBSP fitness or because SAP11$_{MBSP}$ alleles that destabilize other maize TCPs may not be selected in MBSP populations because maize TCPs do not impact *D. maidis* fitness. Finally, both *D. maidis* and MBSP predominantly colonize maize, whereas *M. quadrilineatus* and AYWB colonize a wide range of plants species presenting the possibility that a positive effect of SAP11 on insect fecundity may

have more benefit for a generalist phytoplasma and insect vector than for more specialized ones.

In conclusion, we found that SAP11 effectors of AY-WB and MBS phytoplasmas have evolved to target overlapping but distinct class II TCPs of their plant hosts and that these transcription factors also have overlapping but distinct roles in regulating development in these plant species. In addition, TCPs may or may not impact plant defence responses to phytoplasma leafhopper vectors. The distinct roles of TCPs in regulating plant developmental and defence networks are likely to shape SAP11 effector evolution of phytoplasma.

Material and Methods

Generation of Gateway™ compatible entry clones

We generated Gateway™ compatible entry clones for all experiments, except for the constructs to transform maize. The cloning of the codon-optimized version of $SAP11_{AYWB}$ without the sequence corresponding to the signal peptide into pDONR207 is described previously [8]. The cloning of sequences corresponding to the open reading frames (ORFs) of AtTCP2, AtTCP3, AtTCP4, AtTCP5, AtTCP7, AtTCP10, AtTCP13 and AtTCP17 (S4 Table) into pDONR207 was also done previously [7]. The full-length ORF of AtTCP6, AtTCP8, AtTCP9, AtTCP12, AtTCP14 and AtTCP18 (S4 Table) were PCR amplified from complementary DNA (cDNA) with gene-specific primers that contain partial sequences of the attB1 and attB2 Gateway™ recombination sites (S7 Table). The fragments were further amplified with attB1 and attB2 adapter primers and cloned into pDONR207 with Gateway™ BP Clonase II Enzyme Mix (Invitrogen, Carlsbad, USA). Gateway™ compatible pENTR/SD/D/TOPO vectors containing the full length ORFs of ZmTCP01 (clone UT5707), ZmTCP02 (clone UT5978), ZmTCP05 (clone UT1680), ZmTCP12 (clone UT6182), ZmTCP13 (clone UT3439) and ZmTCP18 (clone UT4097) were ordered from The

Arabidopsis Information Resource (TAIR) (S4 Table). A codon-optimized version of $SAP11_{MBSP}$ without the sequence corresponding to the signal peptide and DNA sequences corresponding to the TCP domains of ZmTCP9, AtTCP12, AtTCP18 and the AtTCP chimeras were gene synthesized by Genscript (New Jersey, USA) with Gateway™ compatible attL1 and attL2 attachment sites (S4 and S8 Tables) and provided in pMS (Genscript).

Transient expression assays in *Arabidopsis thaliana* and maize (Zea mays L.) protoplasts

All genes were transferred from the Gateway™ compatible entry clones into the respective expression vectors with the Gateway™ LR Clonase II enzyme mix (Invitrogen). Full-length ORFs of all TCPs were cloned into pUGW15 [64] to produce N-terminally HA-tagged proteins. The codon-optimized versions of $SAP11_{AYWB}$ and $SAP11_{MBSP}$ without signal peptide sequences were cloned into pUBN-GFP-DEST [65] to produce N-terminally GFP-tagged $SAP11_{AYWB}$ and $SAP11_{MBSP}$. To generate a plasmid for expression of GFP alone, the ccdB cassette of pUBN-GFP-DEST was replaced with a GFP sequence that carries two translational stop codons instead of the translational start codon. The GFP-sequence was amplified from pUBN-GFP-DEST with the gene-specific primers STOP-GFP forward and reverse (S7 Table), cloned into pDONR207 with the Gateway™ BP Clonase II Enzyme Mix (Invitrogen) and transferred to pUBN-GFP-DEST using the Gateway™ LR Clonase II Enzyme Mix (Invitrogen).

Isolation and transformation of Arabidopsis and maize protoplasts were performed as described by [66]. Protoplasts were generated from 6-week-old Arabidopsis and four-leaf stage maize plants grown in controlled environmental conditions with a 14h, 22 C°/ 10h, 20°C light / dark period. The maize plants were transferred into dark for five days before protoplast isolation. 600-µl-protoplast-suspensions were transformed with the indicated

448 constructs and placed in the dark for 12h for gene expression. Protoplasts were harvested by
449 mild centrifugation (1 min, 200 x g) and mixed with 20µl 2X sodium dodecyl sulfate (SDS)-
450 polyacrylamide gel electrophorese (PAGE) sample buffer (50mM Tris/HCl, 10% (w:v) SDS,
451 50% (v:v) glycerol, 0.02% bromophenolblue, 10% ß-mercaptoethanol, pH=6.8). Samples
452 were separated in an SDS-PAGE using 15% SDS-polyacrylamide gels and blotted on 0.45µm
453 BA85 Whatman® Protran® nitrocellulose membranes (Sigma-Aldrich) with the BioRad
454 (Life Science, Hemel Hempstead, UK) minigel and blotting system. Proteins were detected
455 via western blot hybridization with specific antibodies. For detection of GFP-fusion proteins,
456 anti-GFP polyclonal primary antibody (Santa Cruz Biotechnology, Dalla, USA, catalog
457 number: sc-8334, diluted 1:1000) and anti-rabbit-HRP secondary antibody (Sigma-Aldrich,
458 diluted 1:10000) were used. After the anti GFP-antibodies were removed by treatment of the
459 membrane with 0.2 M glycine, 0.1% SDS, 100 mM ß-mercaptoethanol, pH=2, the HA-fusion
460 proteins were detected on the same blot with anti-HA11 monoclonal primary antibody
461 (Covance, New Jersey, USA, order number: MMS-101P, diluted 1:1000) and anti-mouse-
462 HRP secondary antibody (Sigma-Aldrich, diluted 1:10000).
463
464 **Yeast Two-Hybrid analyses**
465 All genes were transferred from the above generated Gateway™ compatible entry
466 clones into the respective Yeast Two-Hybrid vectors with the Gateway™ LR Clonase II
467 enzyme mix (Invitrogen). The codon-optimized sequences corresponding to mature proteins
468 (without signal peptides) of $SAP11_{AYWB}$ and $SAP11_{MBSP}$ were transferred into pDEST-GAD-
469 T7 [67]. The TCP sequences encoding for full length TCPs or TCP domains were transferred
470 into the pDEST-GBK-T7 [67]. *Saccharomyces cerevisiae* strain AH109 (Matchmaker III;
471 Clonetech Laboratories, Mountain View, CA, USA) was transformed using a 96-well
472 transformation protocol [68] and interaction studies were carried out on media depleted of

473 leucine, tryptophan and histidine with addition of 20 mM 3-Amino-1,2,4-triazole (3AT) to
474 suppress auto activation.
475
476 **Generation and analysis of transgenic *A. thaliana* lines**
477 The generation and analysis of the 35S::SAP11$_{AYWB}$ Arabidopsis Col-0 lines, was
478 described previously [8]. Idan Efroni (Weizmann Institute of Science, Rehovot, Israel)
479 provided seeds of the 35S::miR319a x 35S::miR3TCP Arabidopsis Col-0 lines described in
480 Efroni *et al*. [30] and Pilar Cubas (Centro Nacional de Biotecnologia, Madrid, Spain)
481 provided seeds of the *brc1 brc2* Arabidopsis Col-0 line described in Aguilar-Martinez *et al*.
482 [34]. For generation of the 35S::SAP11$_{MBSP}$ Arabidopsis Col-0 lines the codon optimized
483 version of the *SAP11$_{MBSP}$* sequence without the sequence corresponding to the signal peptide
484 was transferred from the Gateway™ compatible entry clone (described above) into the
485 pB7WG2 binary vector using the Gateway™ LR Clonase II Enzyme Mix (Invitrogen) and
486 Arabidopsis Col-0 plants were transformed using the floral dipping method [69].
487
488 **Quantitative Real Time-PCR experiments**
489 SAP11 transcript levels in 35S::SAP11$_{AYWB}$ and 35S::SAP11$_{MBSP}$ *A. thaliana* plants
490 were quantified in mature leaves of three independent, 5-week-old plants. Total RNAs were
491 extracted from 100 mg snap frozen *A. thaliana* leaves with TRI-reagent (Sigma Aldrich) and
492 cDNA synthesis was performed from 0.5 µg total RNA using the M-MLV-reverse
493 transcriptase (Invitrogen). cDNA was subjected to qRT-PCR using SYBR® Green
494 JumpStart™ Taq ReadyMix™ (Sigma-Aldrich) in a CFX96 Touch™ Real-Time PCR
495 Detection System (Biorad) using gene-specific primers for the SAP11-homologs and Actin 2
496 (AT3G18780) (S9 Table).
497

498 **Root length measurements**

499 *A. thaliana* seeds were sterilized in 5% sodium hypochlorite for 8 minutes and washed
500 five times with sterile water. Seeds were germinated on ½ x MS medium with 0.8% (w/v)
501 agar. Three days after germination, seedlings were transferred to ½ x Hoagland medium [70]
502 with 0.25 mM KH_2PO_4 containing 1% (w/v) sucrose and 1% (w/v) agar [41]. Plates were
503 placed vertical to allow root growth on the agar surface. After an additional growth period of
504 10 days seedlings were removed from the plates individually and their root length measured
505 using a ruler.

506

507 **Generation and analysis of transgenic maize lines**

508 Codon optimized versions of the $SAP11_{AYWB}$ and the $SAP11_{MBSP}$ sequences without
509 sequences corresponding to the signal peptide including a sequence encoding an N-terminal
510 3xFLAG-tag were synthesized with flanking BamH1 and EcoRI restriction sites (S10 Table)
511 that were used for cloning into the multiple cloning site of the p1u Vector (DNA Cloning
512 Service, Hamburg, Germany). The resulting *Ubi::FLAG-SAP11-nos* cassette was transferred
513 from p1U into the binary Vector p7i (DNA Cloning Service, Hamburg, Germany) via SfiI
514 restriction sites. Agrobacterium-mediated transformation of maize HiIIAxHiIIB embryos was
515 performed by Crop Genetic Systems (CGS) UG (Hamburg, Germany). T_0 transgenic
516 HiIIAxHiIIB plants were selected with BASTA (Bayer CropScience, Monheim, Germany).
517 For seed reproduction T_0 transgenic plants were crossed with HiIIA plants because the
518 described defects in sexual organs development (Fig. 5) impeded self-pollination. Plants were
519 analyzed for production of proteins from transgenes via western blot hybridizations
520 (explained above) with anti-FLAG M2 monoclonal primary antibody (Sigma-Aldrich, order
521 number: F3165, diluted 1:1000) and anti-mouse-HRP secondary antibody (Sigma-Aldrich,
522 diluted 1:10000) and then used for experiments.

523

524 **Insect fecundity assays**

525 Plants were grown under controlled environmental conditions with a 14h, 22 C°/ 10h,
526 20°C light / dark period for Arabidopsis and 16h, 26°C/ 8h, 20°C light/dark period for maize.
527 Seven-week-old Arabidopsis and three-week-old maize plants were individually exposed to
528 10-15 adult *M. quadrilineatus* or *D. maidis* insects (7-10 females and 3-5 males) for 3 days.
529 The insects were removed and progeny (nymphs or adults) were counted four weeks later.

530

531 **RNA-seq analysis**

532 Fully expanded leaves of seven-week-old *A. thaliana* Col-0 wt and transgenic plants
533 were exposed to five adult *M. quadrilineatus* (2 males and 3 females) in a single clip cage
534 with one clip-cage per plant. For the generation of non-treated samples, clip-cages were
535 applied without insects. After 48h the areas covered by the clip-cages were harvested, snap
536 frozen in liquid nitrogen and stored at -80C until further processing for RNA extraction. For
537 maize, complete three-week-old maize HiIIA wild type (WT) or transgenic plants were
538 exposed to 50 adult *M. quadrilineatus* or *D. maidis* insects (20 males and 30 females) for 48
539 hours and the complete above soil plant material was harvested, snap frozen in liquid
540 nitrogen and stored at -80C until further processing for RNA extraction.

541 Total RNA was extracted from ground Arabidopsis leaf tissue and from 200 mg ground
542 maize material using the RNeasy plant mini kit with on-column DNase digestion (Qiagen).
543 The RNA-seq data of the *A. thaliana* experiments were generated at Academia Sinica
544 (Taipei, Taiwan) and at the Earlham Institute (EI, Norwich, UK). The RNA-seq data of all
545 maize experiments were generated at EI. At Academia Sinica, libraries were generated with
546 the llumina Truseq strand-specific mRNA library preparation without size selection, and
547 sequenced on the Illumina HiSeq2500, 125-bp paired-end reads (YOURGENE Bioscience,

New Taipei City, Taiwan). Libraries at EI were generated using NEXTflex directional RNA library (HT) preparation (Perkin Elmer, Austin, Texas, USA) and sequencing was done on the Illumina HiSeq4000, 75-bp paired-end reads (EI). To assess if the RNA-seq data for the *A. thaliana* experiments received from EI and Academia Sinica are comparable, four samples were sequenced at both facilities. Principal Component Analysis (PCA) showed that the samples generated by these two facilities cluster together demonstrating that batch effects are negligible (S6 Fig.).

The adapter sequences of the raw RNAseq reads were removed using Trim Galore, version 0.4.4 (https://www.bioinformatics.babraham.ac.uk/projects/trim_galore/). The paired-end reads were aligned to the reference genome (*A. thaliana*/TAIR 10.23 and *Z. mays*/AGPv4) with the software TopHat, version 2.1.1 [71]. The number of aligned reads per gene was calculated using HTSeq, version 0.6.1 [72], and data were initially analysed via PCA, using the R/Bioconductor package DESeq2 [73]. Obvious outliers were excluded from the analysis; this amounted to one sample per experiment, as follows: one wild type (WT) Col-0 + *M. quadrilineatus* sample from the *A. thaliana* experiment; one *Ubi::FLAG-SAP11*$_{AYWB}$ + *M. quadrilineatus* sample from one of the maize experiments; one *Ubi::FLAG-SAP11*$_{AYWB}$ + *D. maidis* sample from the other maize experiment; and one *Ubi::FLAG-SAP11*$_{MBSP}$ sample in common with both experiments (S7 Fig., S1, S5, S6 Tables). Differential expression analysis was conducted with DESeq2, using the function -contrast- to make specific comparisons. For further analyses we selected genes that satisfy 3 criteria: *p* value <0.05 after accounting for a 5% false discovery rate (FDR) (Benjamini-Hochberg corrected), mean gene expression value >10 and fold change in expression >2. Cluster analysis was performed on z-score normalized data using the hierarchical method [74].

Transcriptome assemblies of *M. quadrilineatus* and *D. maidis* RNA-seq data

RNA-seq data of *M. quadrilineatus* and *D. maidis* males and females (~25 million reads each) were downloaded from NCBI, accession number SRP093182 and SRP093180 respectively. The reads were used for *de novo* assemblies of male and female transcriptomes separately. Reads were trimmed to remove adaptor sequence and low-quality reads using Trim Galore (https://www.bioinformatics.babraham.ac.uk/projects/trim_galore/). Reads over 20-bp in length were retained for downstream analysis. Trimmed reads were *de novo* assembled using Trinity r20140717 [75] allowing a minimum contig length of 200 bp and minimum k-mer coverage of 2 with default parameters. Assembled contigs were made non-redundant and lowly expressed contigs were filtered with FPKM cut-off 1 using build-in Perl script provided by Trinity. This resulted in 48474 transcripts for male *M. quadrilineatus*, 44409 transcripts for female *M. quadrilineatus*, 42815 transcripts for male *D. maidis* and 59131 transcripts for female *D. maidis*. These assemblies were used to validate the origin of RNA-seq data by assessing if reads aligning to leafhopper transcripts were present in RNA-seq data derived from plants exposed to the leafhoppers as opposed to those of plants that were not exposed to the leafhoppers.

Acknowledgments

We acknowledge Dr. Idan Efroni (Department of Plant Sciences, Weizmann Institute of Science, Rehovot, Israel) for providing seeds for the *35S::miR319a x 35S::miR3TCP* Arabidopsis Col-0 line [30], Dr. Pilar Cubas (Department of Plant Molecular Genetics, Centro Nacional de Biotecnologia, Madrid, Spain) for seeds of the *brc1 brc2* Arabidopsis Col-0 line [34], Dr. Ali Al-Subhi and Prof. Abdullah Al-Saadi (Department of Crop Sciences, Sultan Qaboos University, Muscat, Oman) for assistance with yeast two-hybrid experiments. We thank Dr. Ian Bedford, Anna Jordan, Gavin Hatt and Jake Stone from the JIC entomology team for insect rearing, and Andrew Davis for photography. We also thank Dr. Dirk Becker

(Crop Genetic Systems, Hamburg, Germany) for providing maize HiIIA seeds and Dr. Dirk Becker and Dr. Uta Paszkovski (Department of Plant Sciences, University of Cambridge, Cambridge, UK) for sharing their expertise in maize cultivation. For revision of the manuscript we thank Prof. Richard Immink.

References

1. Weisburg WG, Tully JG, Rose DL, Petzel JP, Oyaizu H, Yang D, *et al*. A phylogenetic analysis of the mycoplasmas: basis for their classification. Journal of Bacteriology. 1989;171(12):6455-67.
2. Gundersen DE, Lee IM, Rehner SA, Davis RE, Kingsbury DT. Phylogeny of mycoplasmalike organisms (Phytoplasmas): a basis for their classification. Journal of Bacteriology. 1994;176(17):5244-54.
3. Lee IM, Davis RE, Gundersen-Rindal DE. Phytoplasma: phytopathogenic mollicutes. Annu Rev Microbiol. 2000;54:221-55.
4. Weintraub PG, Beanland L. Insect vectors of phytoplasmas. Annu Rev Entomol. 2006;51:91-111.
5. Bertaccini A. Phytoplasmas: diversity, taxonomy, and epidemiology. Front Biosci. 2007;12:673-89.
6. Hogenhout SA, Oshima K, Ammar el D, Kakizawa S, Kingdom HN, Namba S. Phytoplasmas: bacteria that manipulate plants and insects. Mol Plant Pathol. 2008;9(4):403-23.
7. Sugio A, MacLean AM, Kingdom HN, Grieve VM, Manimekalai R, Hogenhout SA. Diverse targets of phytoplasma effectors: from plant development to defense against insects. Annu Rev Phytopathol. 2011;49:175-95.

622 8. Sugio A, Kingdom HN, MacLean AM, Grieve VM, Hogenhout SA. Phytoplasma
623 protein effector SAP11 enhances insect vector reproduction by manipulating plant
624 development and defense hormone biosynthesis. Proc Natl Acad Sci U S A.
625 2011;108(48):E1254-63.
626 9. MacLean AM, Orlovskis Z, Kowitwanich K, Zdziarska AM, Angenent GC, Immink
627 RG, *et al*. Phytoplasma effector SAP54 hijacks plant reproduction by degrading
628 MADS-box proteins and promotes insect colonization in a RAD23-dependent
629 manner. PLoS Biol. 2014;12(4):e1001835.
630 10. Kitazawa Y, Iwabuchi N, Himeno M, Sasano M, Koinuma H, Nijo T, *et al*.
631 Phytoplasma-conserved phyllogen proteins induce phyllody across the Plantae by
632 degrading floral MADS domain proteins. J Exp Bot. 2017;68(11):2799-811.
633 11. Sugio A, MacLean AM, Hogenhout SA. The small phytoplasma virulence effector
634 SAP11 contains distinct domains required for nuclear targeting and CIN-TCP binding
635 and destabilization. New Phytol. 2014;202(3):838-48.
636 12. MacLean AM, Sugio A, Makarova OV, Findlay KC, Grieve VM, Toth R, *et al*.
637 Phytoplasma effector SAP54 induces indeterminate leaf-like flower development in
638 Arabidopsis plants. Plant Physiol. 2011;157(2):831-41.
639 13. Orlovskis Z, Hogenhout SA. A bacterial parasite effector mediates insect vector
640 attraction in host plants independently of developmental changes. Front Plant Sci.
641 2016;7:885.
642 14. Janik K, Mithofer A, Raffeiner M, Stellmach H, Hause B, Schlink K. An effector of
643 apple proliferation phytoplasma targets TCP transcription factors-a generalized
644 virulence strategy of phytoplasma? Mol Plant Pathol. 2017;18(3):435-42.

15. Chang SH, Tan CM, Wu CT, Lin TH, Jiang SY, Liu RC, *et al*. Alterations of plant architecture and phase transition by the phytoplasma virulence factor SAP11. J Exp Bot. 2018;69(22):5389-401.

16. Wang N, Yang H, Yin Z, Liu W, Sun L, Wu Y. Phytoplasma effector SWP1 induces witches' broom symptom by destabilizing the TCP transcription factor BRANCHED1. Mol Plant Pathol. 2018;19(12):2623-34.

17. Bai X, Zhang J, Ewing A, Miller SA, Radek AJ, Shevchenko DV, *et al*. Living with genome instability: the adaptation of phytoplasmas to diverse environments of their insect and plant hosts. J Bacteriol. 2006;188(10):3682-96.

18. Toruño TY, Music MS, Simi S, Nicolaisen M, Hogenhout SA. Phytoplasma PMU1 exists as linear chromosomal and circular extrachromosomal elements and has enhanced expression in insect vectors compared with plant hosts. Mol Microbiol. 2010;77(6):1406-15.

19. Chung WC, Chen LL, Lo WS, Lin CP, Kuo CH. Comparative analysis of the peanut witches'-broom phytoplasma genome reveals horizontal transfer of potential mobile units and effectors. PLoS One. 2013;8(4):e62770.

20. Ku C, Lo WS, Kuo CH. Horizontal transfer of potential mobile units in phytoplasmas. Mob Genet Elements. 2013;3(5):e26145.

21. Lee IM, Gundersen-Rindal DE, Davis RE, Bottner KD, Marcone C, Seemuller E. '*Candidatus* Phytoplasma asteris', a novel phytoplasma taxon associated with aster yellows and related diseases. Int J Syst Evol Microbiol. 2004;54(Pt 4):1037-48.

22. Sugio A, Hogenhout SA. The genome biology of phytoplasma: modulators of plants and insects. Curr Opin Microbiol. 2012;15(3):247-54.

668 23. Nault LR, Delong DM. Evidence for co-evolution of leafhoppers in the genus
669 Dalbulus (*Cicadellidae: Homoptera*) with maize and its ancestors. Annals of the
670 Entomological Society of America. 1980;73(4):349-53.
671 24. Gonzalez JG, Jaramillo MG, Lopes JRS. Undetected infection by maize bushy stunt
672 phytoplasma enhances host-plant preference to *Dalbulus maidis* (*Hemiptera:*
673 *Cicadellidae*). Environmental entomology. 2018;47(2):396-402.
674 25. Navaud O, Dabos P, Carnus E, Tremousaygue D, Herve C. TCP transcription factors
675 predate the emergence of land plants. J Mol Evol. 2007;65(1):23-33.
676 26. Cubas P, Lauter N, Doebley J, Coen E. The TCP domain: a motif found in proteins
677 regulating plant growth and development. The Plant journal : for cell and molecular
678 biology. 1999;18(2):215-22.
679 27. Aggarwal P, Das Gupta M, Joseph AP, Chatterjee N, Srinivasan N, Nath U.
680 Identification of specific DNA binding residues in the TCP family of transcription
681 factors in Arabidopsis. Plant Cell. 2010;22(4):1174-89.
682 28. Martin-Trillo M, Cubas P. TCP genes: a family snapshot ten years later. Trends Plant
683 Sci. 2009;15(1):31-9.
684 29. Howarth DG, Donoghue MJ. Duplications in *Cys*-like genes from Dipsacales
685 correlate with floral form. Int J Plant Sci. 2005;166(3):357-70.
686 30. Efroni I, Blum E, Goldshmidt A, Eshed Y. A protracted and dynamic maturation
687 schedule underlies Arabidopsis leaf development. Plant Cell. 2008;20(9):2293-306.
688 31. Schommer C, Debernardi JM, Bresso EG, Rodriguez RE, Palatnik JF. Repression of
689 cell proliferation by miR319-regulated TCP4. Mol Plant. 2014;7(10):1533-44.
690 32. Nicolas M, Cubas P. The role of TCP transcription factors in shaping flower structure,
691 leaf morphology, and plant architecture. 2015:249-67.

692 33. Vadde BVL, Challa KR, Nath U. The TCP4 transcription factor regulates trichome
693 cell differentiation by directly activating GLABROUS INFLORESCENCE STEMS in
694 *Arabidopsis thaliana*. The Plant journal : for cell and molecular biology.
695 2018;93(2):259-69.
696 34. Aguilar-Martinez JA, Poza-Carrion C, Cubas P. Arabidopsis BRANCHED1 acts as an
697 integrator of branching signals within axillary buds. Plant Cell. 2007;19(2):458-72.
698 35. Koyama T, Furutani M, Tasaka M, Ohme-Takagi M. TCP transcription factors
699 control the morphology of shoot lateral organs via negative regulation of the
700 expression of boundary-specific genes in Arabidopsis. Plant Cell. 2007;19(2):473-84.
701 36. Gonzalez-Grandio E, Poza-Carrion C, Sorzano CO, Cubas P. BRANCHED1
702 promotes axillary bud dormancy in response to shade in Arabidopsis. Plant Cell.
703 2013;25(3):834-50.
704 37. Yang Y, Nicolas M, Zhang J, Yu H, Guo D, Yuan R, *et al*. The TIE1 transcriptional
705 repressor controls shoot branching by directly repressing BRANCHED1 in
706 Arabidopsis. PLoS Genet. 2018;14(3):e1007296.
707 38. Luo D, Carpenter R, Copsey L, Vincent C, Clark J, Coen E. Control of organ
708 asymmetry in flowers of Antirrhinum. Cell. 1999;99(4):367-76.
709 39. Doebley J., Stec A, Gustus C. *teosinte branched1* and the origin of maize: evidence
710 for epistasis and the evolution of dominance. Genetics. 1995;141:333-46.
711 40. Studer AJ, Wang H, Doebley JF. Selection during maize domestication targeted a
712 gene network controlling plant and inflorescence architecture. Genetics.
713 2017;207(2):755-65.
714 41. Lu YT, Li MY, Cheng KT, Tan CM, Su LW, Lin WY, *et al*. Transgenic plants that
715 express the phytoplasma effector SAP11 show altered phosphate starvation and
716 defense responses. Plant Physiol. 2014;164(3):1456-69.

42. Burdo B, Gray J, Goetting-Minesky MP, Wittler B, Hunt M, Li T, *et al*. The Maize TFome--development of a transcription factor open reading frame collection for functional genomics. The Plant journal : for cell and molecular biology. 2014;80(2):356-66.

43. Yilmaz A, Nishiyama MY, Jr., Fuentes BG, Souza GM, Janies D, Gray J, *et al*. GRASSIUS: a platform for comparative regulatory genomics across the grasses. Plant Physiol. 2009;149(1):171-80.

44. Bai F, Reinheimer R, Durantini D, Kellogg EA, Schmidt RJ. TCP transcription factor, BRANCH ANGLE DEFECTIVE 1 (BAD1), is required for normal tassel branch angle formation in maize. Proc Natl Acad Sci U S A. 2012;109(30):12225-30.

45. Chai W, Jiang P, Huang G, Jiang H, Li X. Identification and expression profiling analysis of TCP family genes involved in growth and development in maize. Physiol Mol Biol Plants. 2017;23(4):779-91.

46. Hubbard L, McSteen P, Doebley J, Hake S. Expression patterns and mutant phenotype of *teosinte branched1* correlate with growth suppression in maize and teosinte. Genetics. 2002;162(4):1927-35.

47. Brown PJ, Upadyayula N, Mahone GS, Tian F, Bradbury PJ, Myles S, *et al*. Distinct genetic architectures for male and female inflorescence traits of maize. PLoS Genet. 2011;7(11):e1002383.

48. Horn S, Pabón-Mora N, Theuß VS, Busch A, Zachgo S. Analysis of the CYC/TB1 class of TCP transcription factors in basal angiosperms and magnoliids. The Plant Journal. 2014;81(4):559-71.

49. Finlayson SA. Arabidopsis TEOSINTE BRANCHED1-LIKE 1 regulates axillary bud outgrowth and is homologous to monocot TEOSINTE BRANCHED1. Plant Cell Physiol. 2007;48(5):667-77.

742 50. Dong Z, Li W, Unger-Wallace E, Yang J, Vollbrecht E, Chuck G. Ideal crop plant
743 architecture is mediated by *tassels replace upper ears1*, a BTB/POZ ankyrin repeat
744 gene directly targeted by TEOSINTE BRANCHED1. Proc Natl Acad Sci U S A.
745 2017;114(41):E8656-e64.
746 51. Gonzalez-Grandio E, Pajoro A, Franco-Zorrilla JM, Tarancon C, Immink RG, Cubas
747 P. Abscisic acid signaling is controlled by a BRANCHED1/HD-ZIP I cascade in
748 Arabidopsis axillary buds. Proc Natl Acad Sci U S A. 2017;114(2):E245-E54.
749 52. Niwa M, Daimon Y, Kurotani K, Higo A, Pruneda-Paz JL, Breton G, *et al*.
750 BRANCHED1 interacts with FLOWERING LOCUS T to repress the floral transition
751 of the axillary meristems in Arabidopsis. Plant Cell. 2013;25(4):1228-42.
752 53. Niwa M, Endo M, Araki T. Florigen is involved in axillary bud development at
753 multiple stages in Arabidopsis. Plant signaling & behavior. 2013;8(11):e27167.
754 54. Maejima K, Iwai R, Himeno M, Komatsu K, Kitazawa Y, Fujita N, *et al*. Recognition
755 of floral homeotic MADS domain transcription factors by a phytoplasmal effector,
756 phyllogen, induces phyllody. The Plant journal : for cell and molecular biology.
757 2014;78(4):541-54.
758 55. Maejima K, Kitazawa Y, Tomomitsu T, Yusa A, Neriya Y, Himeno M, *et al*.
759 Degradation of class E MADS-domain transcription factors in Arabidopsis by a
760 phytoplasmal effector, phyllogen. Plant signaling & behavior. 2015;10(8):e1042635.
761 56. Orlovskis Z, Canale MC, Haryono M, Lopes JRS, Kuo CH, Hogenhout SA. A few
762 sequence polymorphisms among isolates of Maize bushy stunt phytoplasma associate
763 with organ proliferation symptoms of infected maize plants. Ann Bot.
764 2017;119(5):869-84.
765 57. Palatnik JF, Edwards A, Wu X, Schommer C, Schwab R, Carrington JC, *et al*.
766 Control of leaf morphogenesis by microRNAs. Nature. 2003;425.

767 58. Schommer C, Palatnik JF, Aggarwal P, Chetelat A, Cubas P, Farmer EE, *et al*.
768 Control of jasmonate biosynthesis and senescence by miR319 targets. PLoS Biol.
769 2008;6(9):e230.
770 59. Sarvepalli K, Nath U. Hyper-activation of the TCP4 transcription factor in
771 *Arabidopsis thaliana* accelerates multiple aspects of plant maturation. The Plant
772 journal : for cell and molecular biology. 2011;67(4):595-607.
773 60. Danisman S, van der Wal F, Dhondt S, Waites R, de Folter S, Bimbo A, *et al*.
774 Arabidopsis class I and class II TCP transcription factors regulate jasmonic acid
775 metabolism and leaf development antagonistically. Plant Physiol. 2012;159(4):1511-
776 23.
777 61. Zhang C, Ding Z, Wu K, Yang L, Li Y, Yang Z, *et al*. Suppression of Jasmonic Acid-
778 Mediated Defense by Viral-Inducible MicroRNA319 Facilitates Virus Infection in
779 Rice. Mol Plant. 2016;9(9):1302-14.
780 62. Yang L, Teixeira PJ, Biswas S, Finkel OM, He Y, Salas-Gonzalez I, *et al*.
781 *Pseudomonas syringae* type III effector HopBB1 promotes host transcriptional
782 repressor degradation to regulate phytohormone responses and virulence. Cell Host
783 Microbe. 2017;21(2):156-68.
784 63. Jiao Y, Lee YK, Gladman N, Chopra R, Christensen SA, Regulski M, *et al*. MSD1
785 regulates pedicellate spikelet fertility in sorghum through the jasmonic acid pathway.
786 Nat Commun. 2018;9(1):822.
787 64. Nakagawa T, Ishiguro S, Kimura T. Gateway vectors for plant transformation. Plant
788 Biotech. 2009:275-84.
789 65. Grefen C, Donald N, Hashimoto K, Kudla J, Schumacher K, Blatt MR. A ubiquitin-
790 10 promoter-based vector set for fluorescent protein tagging facilitates temporal

stability and native protein distribution in transient and stable expression studies. The Plant journal : for cell and molecular biology. 2010;64(2):355-65.

66. Yoo SD, Cho YH, Sheen J. Arabidopsis mesophyll protoplasts: a versatile cell system for transient gene expression analysis. Nat Protoc. 2007;2(7):1565-72.

67. Rossignol P, Collier S, Bush M, Shaw P, Doonan JH. Arabidopsis POT1A interacts with TERT-V(I8), an N-terminal splicing variant of telomerase. J Cell Sci. 2007;120(Pt 20):3678-87.

68. Pecher P, Eschen-Lippold L, Herklotz S, Kuhle K, Naumann K, Bethke G, *et al*. The *Arabidopsis thaliana* mitogen-activated protein kinases MPK3 and MPK6 target a subclass of 'VQ-motif'-containing proteins to regulate immune responses. New Phytol. 2014;203(2):592-606.

69. Logemann E, Birkenbihl RP, Ulker B, Somssich IE. An improved method for preparing Agrobacterium cells that simplifies the Arabidopsis transformation protocol. Plant Methods. 2006;2:16.

70. Hoagland DR, Arnon DI. The water-culture method for growing plants without soil. California Agri- cultural Experimental Station Circular 1950;347:1-39.

71. Kim D, Pertea G, Trapnell C, Pimentel H, Kelley R, Salzberg SL. TopHat2: accurate alignment of transcriptomes in the presence of insertions, deletions and gene fusions. Genome biology. 2013;14(4):R36.

72. Anders S, Pyl PT, Huber W. HTSeq--a Python framework to work with high-throughput sequencing data. Bioinformatics (Oxford, England). 2015;31(2):166-9.

73. Love MI, Huber W, Anders S. Moderated estimation of fold change and dispersion for RNA-seq data with DESeq2. Genome biology. 2014;15(12):550.

74. Murtagh F, Legendre P. Ward's hierarchical agglomerative clustering method : which algorithms implement Ward's criterion? Journal of Classification. 2014;31:274-95.

816 75. Grabherr MG, Haas BJ, Yassour M, Levin JZ, Thompson DA, Amit I, *et al*. Full-
817 length transcriptome assembly from RNA-Seq data without a reference genome.
818 Nature biotechnology. 2011;29(7):644-52.

819

820 ## Figure Captions

821 **Fig. 1. $SAP11_{AYWB}$ and $SAP11_{MBSP}$ interactions with *A. thaliana* TCP transcription**
822 **factors.** (A) Western blots of *A. thaliana* protoplast destabilization assays; $SAP11_{AYWB}$ and
823 $SAP11_{MBSP}$ destabilize the CYC/TB1 TCPs BRC1 (AtTCP18) and BRC2 (AtTCP12) and
824 $SAP11_{AYWB}$ also all class II CIN-TCPs, whereas the SAP11 homologs did not destabilize
825 class I TCPs. GFP-tagged SAP11 (filled arrowheads) or GFP alone (open arrowheads) and
826 HA-tagged TCPs were detected with specific antibodies to GFP and HA, respectively, as
827 indicated at left of the blots. *band of the correct size in case of multiple bands on the blots.
828 Loading controls: Amidoblack-stained large RUBISCO subunit. (B) Yeast two-hybrid assays
829 of interactions of $SAP11_{AYWB}$ with CIN and CYC/TB1-TCPs and $SAP11_{MBSP}$ with
830 CYC/TB1-TCPs. Positive interactions are visible by yeast growth on SD-LWH selection
831 media containing 20 mM 3-Amino-1,2,4-triazole (3AT). EV=empty vector controls showing
832 absence of auto activations. (C) qRT-PCRs of transcripts of $SAP11_{AYWB}$ and $SAP11_{MBSP}$
833 transgenes in *A. thaliana* lines shown in D-F. *$p<0.01$, students t-test compared to Col-0,
834 n=3. (D-G) *35S::*$SAP11_{AYWB}$ stable transgenic *A. thaliana* (Col-0) lines phenocopy both the
835 *A. thaliana brc1-2 brc2-1* (*brc1 brc2*) double (Col-0) mutant and *35S::miR319a x*
836 *35S::miR3TCP* stable transgenic *A. thaliana* (Col-0) lines and *35S::*$SAP11_{MBSP}$ transgenic
837 lines phenocopy only the *A. thaliana brc1 brc2* mutant. Nine-week-old plants were
838 phenotyped for rosette leaf morphology (D), overall appearance of side views (E), rosette
839 diameters (F) and numbers of primary branches emerging from the rosettes (G). (F, G) Error

840 bars denote standard errors (n=24). Letters indicate groups that are statistically different (one-
841 way ANOVA with Tukey´s Multiple Comparison Test).
842
843 **Fig. 2. SAP11 binding specificity to regions within the TCP domains of *A. thaliana***
844 **TCP2 (CIN-TCP) and TCP18 (CYC/TB1-TCP BRC1).** (A) Aligned amino acid sequences
845 of the TCP domains of TCP2 and TCP18 with boxed basic and helix-loop-helix domains.
846 (B) Binding specificity of $SAP11_{MBSP}$ requires the complete TCP18 helix-loop-helix domain.
847 Schematic representation at left are the 59-amino-acid TCP2 and TCP18 TCP domain
848 chimeras and AtTCP2 and AtTCP18 wildtype TCP domains tested for $SAP11_{AYWB}$ or
849 $SAP11_{MBSP}$ binding in yeast two-hybrid analysis at right, as described in the Fig. 1 legend.
850
851 **Fig. 3 Analyses of the impact of phytoplasma $SAP11_{AYWB}$ and $SAP11_{MBSP}$ effectors on**
852 ***A. thaliana* susceptibility to the AY-WB insect vector *M. quadrilineatus*.** (A) $SAP11_{AYWB}$
853 promotes *M. quadrilineatus* nymph production on *A. thaliana*, whereas $SAP11_{MBSP}$ does not.
854 Error bars denote standard errors, *p<0.01, students t-test compared to Col-0, n=3.
855 (B) Principal component analysis (PCA) on the matrix of normalized read counts of 6
856 treatments (n=3-4, see S1 Table) showing that $SAP11_{AYWB}$ modulates plant responses to
857 *M. quadrilineatus* (+Mq) differently compared to $SAP11_{MBSP}$ and wt *A. thaliana* (Col-0).
858 (C, D) Volcano plots showing differentially expressed genes (DEGs) in insect exposed
859 $Sap11_{AYWP}$ and $SAP11_{MBSP}$. DEGs with potential relevance in SAP11 dependent response
860 (red dots) to *M. quadrilineatus* were selected by three criteria (i) P value > 0.05 (red and blue
861 dots), (ii) average read count > 10 (dashed horizontal line) and (iii) log2 fold change > 1
862 (dashed vertical lines). (E) $SAP11_{AYWB}$ modulates plant defence responses to
863 *M. quadrilineatus* relatively to Col-0, unlike $SAP11_{MBSP}$. Hierarchical clustering based on
864 normalized read counts of 96 selected DEGs (red dots in C). See S2 Table for normalized

865 read count values of all treatments and S3 Table for gene annotations with 30 genes known to
866 be involved in defence highlighted in yellow. All experiments were executed with
867 *35S::SAP11*$_{AYWB}$ line 7 [8] and *35S::SAP11*$_{MBSP}$ line 1 (this work).
868
869 **Fig. 4 Classification of *Z. mays* (Zm) TCPs.** The TCP motifs identified in 44 ZmTCPs
870 (http://grassius.org/grasstfdb.html) were aligned with subgroup specific TCPs from *Oryza*
871 *sativa* (Os) OsPCF1/2, *Antirrhinummajus* CINCINNATA (AmCIN) and CYCLOIDEA
872 (AmCYC) and *Z. mays* TEOSINTE BRANCHED1 (ZmTCP02/TB1) (CYC/TB1 green).
873 A number of proteins carry truncated TCP motifs at their N- or C-terminus (ZmTCP04,
874 ZmTCP06, ZmTCP12, ZmTCP14, ZmTCP20, ZmTCP42 and ZmTCP44) or incomplete
875 versions of the TCP-motif within their amino acid sequence (ZmTCP07, ZmTCP28,
876 ZmTCP43). The ZmTCPs were assigned to the (sub)groups based on amino acid
877 conservations (Class I, yellow; Class II, blue; CIN, red and CYC/TB1, green with AmCYC-
878 like TCPs in purple and TB1-like TCPs in orange) [28] A new CII subgroup shares sequence
879 homology with CIN-TCPs and CYC/TB1-TCPs. Asterisks indicate TCPs with potential
880 miR319a target sites identified in their coding gene sequences (S5 Fig.).
881
882 **Fig. 5 SAP11$_{AYWB}$ and SAP11$_{MBSP}$ interactions with maize TCP transcription factors**
883 **(ZmTCPs).** (A) SAP11$_{AYWB}$ interacts with ZmTCPs of the three Class II subgroups and
884 SAP11$_{MBSP}$ with CYC/TB1 ZmTCPs in yeast two-hybrid (Y2H) experiments. Y2H
885 experiments were executed with full-length ZmTCP proteins, except ZmTCP09 for which the
886 DNA sequence corresponding to the 59 amino-acid of the TCP-motif was synthesized
887 (Genscript). (B) SAP11$_{AYWB}$ and SAP11$_{MBSP}$ destabilize ZmTCPs inside maize protoplasts.
888 Immunoblots show detection of GFP-tagged SAP11 (filled arrowheads) or GFP alone (open
889 arrowheads) and HA-tagged TCPs with specific antibodies to GFP and HA, respectively, as

890 indicated at left of the blots. Loading control: amidoblack staining of the large RUBISCO
891 subunit. (C) For phenotyping FLAG-SAP11$_{AYWB}$ (lane 1) and FLAG-SAP11$_{MBSP}$ (lane 2)
892 were detected in plants of the heterozygous transgenic Ubi::FLAG-SAP11$_{AYWB}$1 and
893 Ubi::FLAG-SAP11$_{MBSP}$1 maize lines. The immunoblots shown were probed with anti-flag
894 antibodies. (D) Severe developmental phenotypes of *Ubi::FLAG-SAP11$_{AYWB}$* (HiIIA) and
895 *Ubi::FLAG-SAP11$_{MBSP}$* (HiIIA) transgenic maize plants. Phenotyping was done on 13-week-
896 old transgenic and WT HiIIA plants; for each transgenic Ubi::FLAG-SAP11 maize line 3
897 plants were analysed and photos of one representative plant are shown. (a-c) Both *SAP11*
898 transgenic lines are shorter and produce more tillers surrounding the main culm compared to
899 WT HiIIA and *SAP11$_{MBSP}$* lines also produced more axillary branches. (d-f) Crinkling of leaf
900 edges at the base of only the *SAP11$_{AYWB}$* lines. (g-i and insets 1-3) Impaired female
901 inflorescence development of both *SAP11* transgenic lines. Red silk like structures emerged
902 from the leaf sheath in the *SAP11$_{AYWB}$* line (h, inset 2) whereas long axillary branches tipped
903 by tassels emerged in the *SAP11$_{MBSP}$* line (i, inset 3), compared to ears in WT HiIIA (g, inset
904 1). *SAP11$_{MBSP}$* plants produced fertile pollen from these tassels, but were female sterile. (j-l,
905 insets 7-11) Impaired male inflorescence development of *SAP11* transgenic lines. *SAP11$_{AYWB}$*
906 lines developed feminized tassel, including the development of silks, at the tip of the main
907 culm (k, inset 8) and at the tip of the tillers (k, inset 9). The tassel development of *SAP11$_{MBSP}$*
908 lines at the tip of the main culm (l, inset 10) and at the tip of tillers (l, inset 11) resembled
909 those of WT HiIIA (j, inset 7). (E) Feminized tassels of *SAP11$_{AYWB}$* lines are fertile.
910 Pollination of feminized tassels (k, insets 8 and 9) with pollen from *SAP11$_{MBSP}$* or WT plants
911 produced kernels (m and n), which germinated (not shown). In addition, pollination of the
912 silks emerging from the leaf sheath (h, inset 2) resulted in the development of naked ears,
913 without husk leaves, emerging directly from the leaf sheath (o). The ears produced kernels

914 (o) that germinated (not shown). The *SAP11*$_{MBSP}$ lines did not produce pollen and therefore
915 are male sterile.
916
917 **Fig. 6 Schematic presentation of phenotyping results of WT maize (*Z. mays*), *tb1* maize**
918 **and *Ubi::FLAG-SAP11* maize plants.** Schematic presentations of the phenotypes of teosinte
919 and *tb1* are included as comparison [39,46,47]. *tb1* resembles teosinte architecture but has
920 impaired development of female inflorescences . *Ubi::FLAG-SAP11*$_{MBSP}$ plants phenocopy
921 *tb1* plants. *Ubi::FLAG-SAP11*$_{AYWB}$ plants produce more tillers with female infloresences and
922 naked ears from the main culm, and are male sterile. Main culms are indicated in black,
923 axillary branches in green, tillers in blue, silks directly emerging from the main culm in red,
924 silks of ears in yellow and inflorescences in symbols (♂ , male; ♀, female).
925
926 **Fig. 7 The phytoplasma SAP11$_{AYWB}$ and SAP11$_{MBSP}$ effectors do not modulate maize**
927 **defences in response to exposure to AYWB and MBSP leafhopper vectors**
928 ***M. quadrilineatus* and *D. maidis*, respectively.** (A, B) Numbers of nymphs produced from
929 the two leafhopper species are similar among *SAP11* transgenic and WT maize lines.
930 AYWB1, 2 and 3 and MBSP1 and 2 indicate independent transgenic lines. a above the error
931 bars indicates no significant differences (one-way ANOVA with Tukey´s Multiple
932 Comparison Test, n=4). (C) *M. quadrilineatus* exposure (+Mq) similarly alters gene
933 expression of *SAP11*$_{AYWB}$ and *SAP11*$_{MBSP}$ transgenic and WT maize lines. (D) Gene
934 expression patterns of *D. maidis*-exposed (+Dm) transgenic and WT maize lines are similar
935 to those of non-exposed lines. (C, D) Principal component analysis (PCA) on the matrix of
936 normalized read counts of 6 treatments (n=3-4 per treatment, see S5 and S6 Tables). RNA-
937 seq experiments were done with *Ubi::FLAG-SAP11*$_{AYWB}$ line 1 and *Ubi::FLAG-SAP11*$_{MBSP}$
938 line 1.

Supporting information captions

S1 Fig. Phenotyping of transgenic *35S::SAP11$_{AYWB}$* and *35S::SAP11$_{MBSP}$* Arabidopsis plants. Three independent lines overexpressing either *SAP11$_{AYWB}$* or *SAP11$_{MBSP}$* were analysed in comparison to Col-0, the *brc1 brc2* mutant and *35S::miR319a x 35S::miR3TCP* with regard to (A) the number of rosette leaves when first bolting buds appeared at the centre of the leaf rosette, (B) the time point of bolting buds appearance, (C) the plant height and (D) the number of primary cauline-leaf branches (CI). The number of primary rosette-leaf branches (RI) are presented in Fig. 1G of the main text. (E) Schematic presentation of Arabidopsis branching. Error bars denote standard errors (n=24). Asterisks indicate statistically significant differences compared to Col-0. (*, $p<0.05$, **, $p<0.01$, ***, $p<0.001$, student´s t-test); ns, not significant.

S2 Fig. CIN-TCP destabilization affects root lengths. (A) Roots of representative *35S::SAP11$_{AYWB}$* and *35S::SAP11$_{MBSP}$* mutants compared to Col-0, the *brc1 brc2* mutant and *35S::miR319a x 35S::miR3TCP* lines. (B) Root length measurements of indicated mutants compared to Col-0. Error bars denote standard errors (n=20). Asterisks indicates statistically significant difference (*, $p<0.001$, student´s t-test); ns, not significant.

S3 Fig. Classification of *Sorghum bicolor* (Sb) TCPs. The TCP motifs of 27 SbTCPs (http://grassius.org/grasstfdb.html) were aligned and assigned to the TCP (sub)groups as described in Fig. 4. Corresponding gene codes are presented in S4 Table. SbTCP4 carries a truncated TCP-motif at its C-terminus and SbTCP10 and SbTCP23 carry incomplete versions of the TCP-motif within their amino acid sequence. Sequences were aligned using ClustalW (http://www.genome.jp/tools/clustalw/) and visualized using the Boxshade software

963 (http://www.ch.embnet.org/software/BOX_form.html). Asterisks indicate TCPs with
964 potential miR319a target sites identified in their coding gene sequences (S5 Fig.).
965
966 **S4 Fig. Classification of *Oryza sativa* (Oz) TCPs.** The TCP motifs of 27 OzTCPs
967 (http://grassius.org/grasstfdb.html) were aligned and assigned to the TCP (sub)groups as
968 described in Fig. 4. Corresponding gene codes are presented in S4 Table. Sequences were
969 aligned using ClustalW (http://www.genome.jp/tools/clustalw/) and visualized using the
970 Boxshade software (http://www.ch.embnet.org/software/BOX_form.html). Asterisks indicate
971 TCPs with potential miR319a target sites identified in their coding gene sequences (S5 Fig.).
972
973 **S5 Fig. Identification of potential miR319a target sites.** The CDS of the TCPs from *Zea*
974 *mays* (Zm), *Oryza sativa* (Os), *Sorghum bicolor* (Sb), and of the *Antirrhinum majus* (Am)
975 CIN-TCP were screened for potential miR319a target sites. They are depicted together with
976 the miR319a binding sites of *Arabidopsis thaliana* (At) CIN-TCPs [57]. Nucleotides known
977 to be involved in miR319a binding to AtCIN-TCPs are indicated in grey [57].
978
979 **S6 Fig. Principal component analysis (PCA) showing that samples sequenced at**
980 **different facilities cluster together (batch effect is negligible).** PCA was conducted with
981 normalized read counts of RNA-seq data obtained from *M. quadrilineatus*-exposed leaves of
982 three *A. thaliana* Col-0 plants (samples #1, 2 and 3) and *35S::miR319a x 35S::miR3TCP*
983 sample #4 generated at the Earlham Institute, Norwich, UK (red circles) and Academia
984 Sinica, Taipei, Taiwan (green triangles).
985
986 **S7 Fig. Cluster analysis performed on the matrix of normalized read counts of RNA-seq**
987 **values from** (A) *Arabidopsis* Col-0, *35S::SAP11*$_{AYWB}$ and *35S::SAP11*$_{MBSP}$ non-exposed and

exposed to *M quadrilineatus* (+Mq). (B) *Z. mays* HiIIA, *Ubi::FLAG-SAP11*$_{AYWB}$ and *Ubi::FLAG-SAP11*$_{MBSP}$ non-exposed and exposed to *M. quadrilineatus* (+Mq) and (C) non-exposed and exposed to *D. maidis* (+Dm). Experiments were done with *35S::SAP11*$_{AYWB}$ line 7 (Sugio *et al.,* 2011b), *35S::SAP11*$_{MBSP}$ line 1, *Ubi::FLAG-SAP11*$_{AYWB}$ line 1 and *Ubi::FLAG-SAP11*$_{MBSP}$ line 1.

S1 Table: Alignment to SAP11 transgene, M. quadrilineatus transcriptome and A. thaliana genome of RNA-seq data shown in Fig. 3. +Mq indicates samples from *M. quadrilineatus* exposed plants.

S2 Table: List of differentially expressed genes and expression values in RNA-seq experiments of 6 treatments. The genes are ordered according to the heat map in Fig 3E. Genes potentially involved in plant defense response are highlighted in yellow and annotations of these genes are listed in S3 Table. +Mq indicates samples from *M. quadrilineatus* exposed plants.

S3 Table: List of differentially expressed genes with potential biological functions. The genes are ordered according to the heat map in Fig 3E. Genes potentially involved in plant defense response are highlighted in yellow.

S4 Table: Sequence IDs of TCPs from Zea mays (Zm), Arabidopsis thaliana (At), Sorghum bicolor (Sb) and Oryza sativa (Os).

S5 Table: Alignment to SAP11 transgene, *M. quadrilineatus* transcriptome and *Z. mays* genome of RNA-seq data of *M. quadrilineatus*-exposed (+Mq) *Z. mays* shown in Fig. 7.

S6 Table: Alignment to SAP11 transgene, *D. maidis* transcriptome and *Z. mays* genome of RNA-seq data of *D. maidis*-exposed (+Dm) *Z. mays* shown in Fig. 7.

S7 Table. Oligonucleotide sequences (5′ > 3′) for cloning.

S8 Table. Synthesized CDS (underlined) flanked by gateway compatible attL1 and attL2 sites. Nucleotide sequences for gene syntheses of $SAP11_{MBSP}$ for expression in *Arabidopsis thalina* and of the TCP domains from *ZmTCP33*, *AtTCP2*, *AtTCP18* and chimeras of *AtTCP2* and *AtTCP18* TCP domains for expression in yeast.

S9 Table. Oligonucleotide sequences (5′ > 3′) for qRT-PCR.

S10 Table. Nucleotide sequences for gene syntheses of *FLAG-SAP11*$_{MBSP}$ and *FLAG-SAP11*$_{AYWB}$ for expression in *Zea mays.* Kodzak sequences are in italic, ORFs are flanked by *Bam*HI and *Eco*R1 restriction sites (grey) for subsequent cloning.

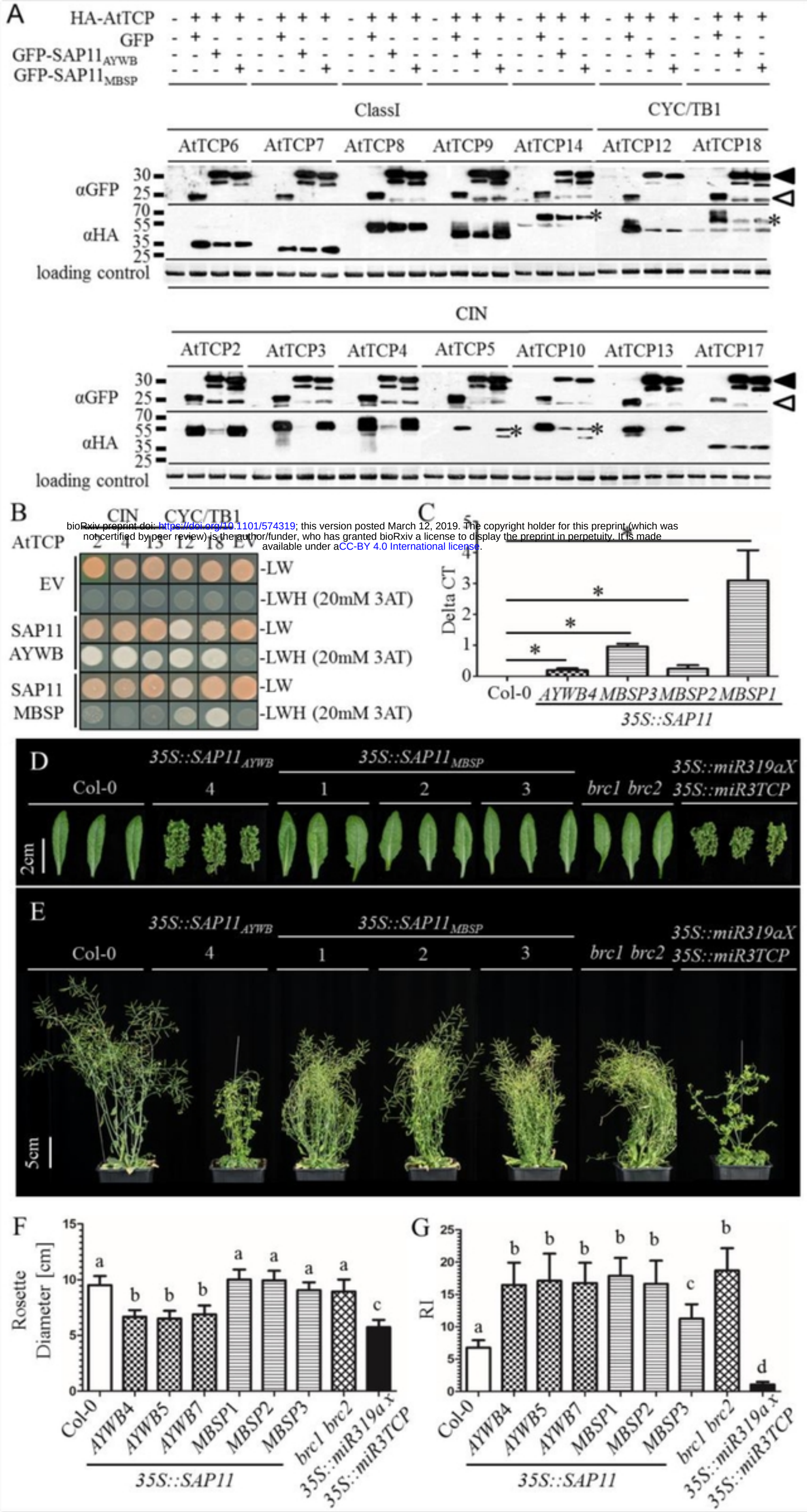

Fig1

A

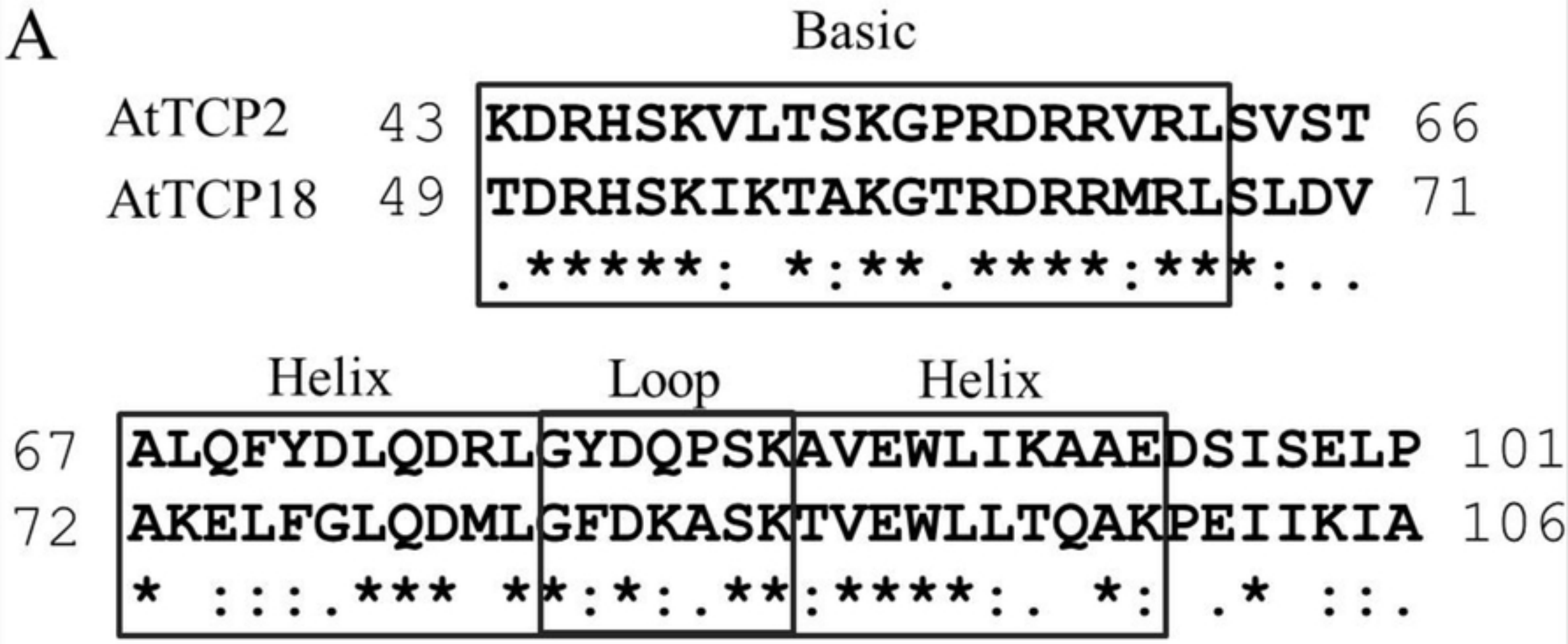

B

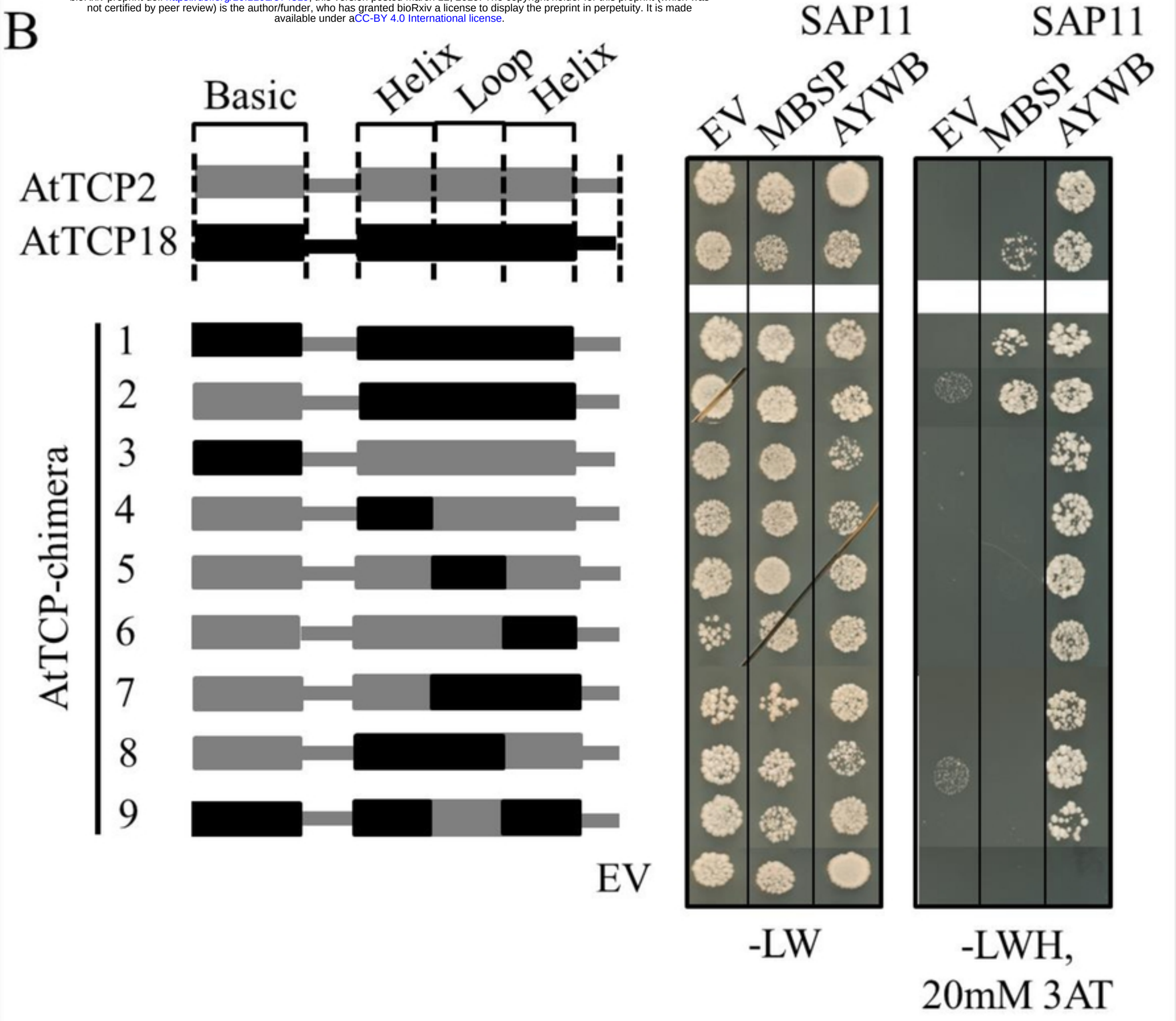

Fig2

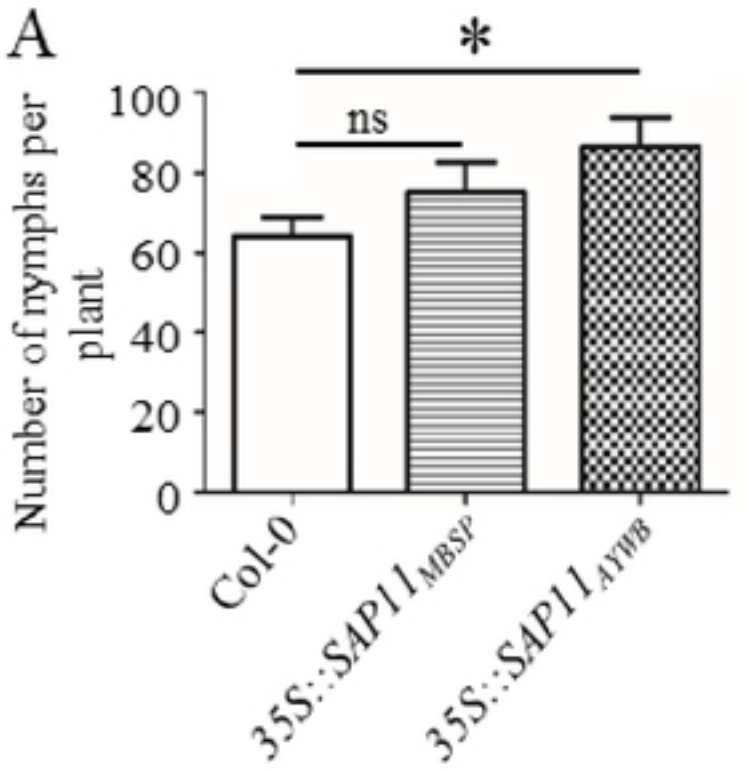

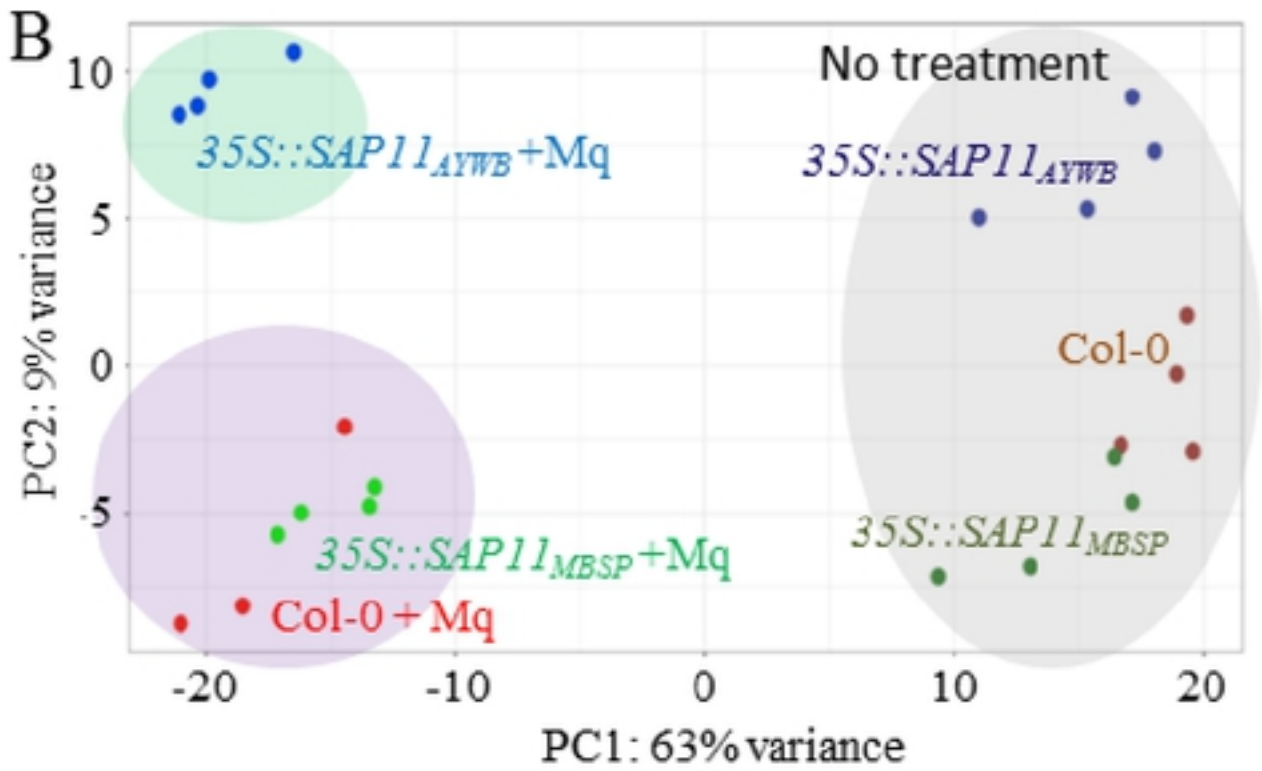

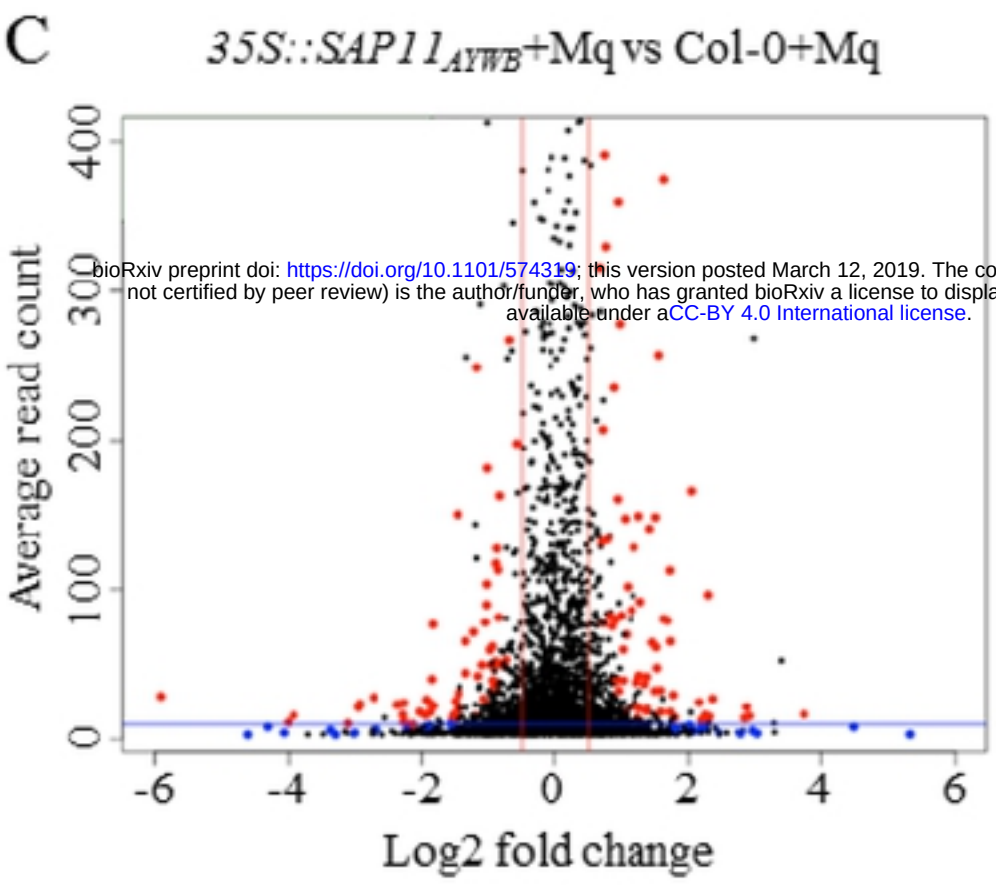

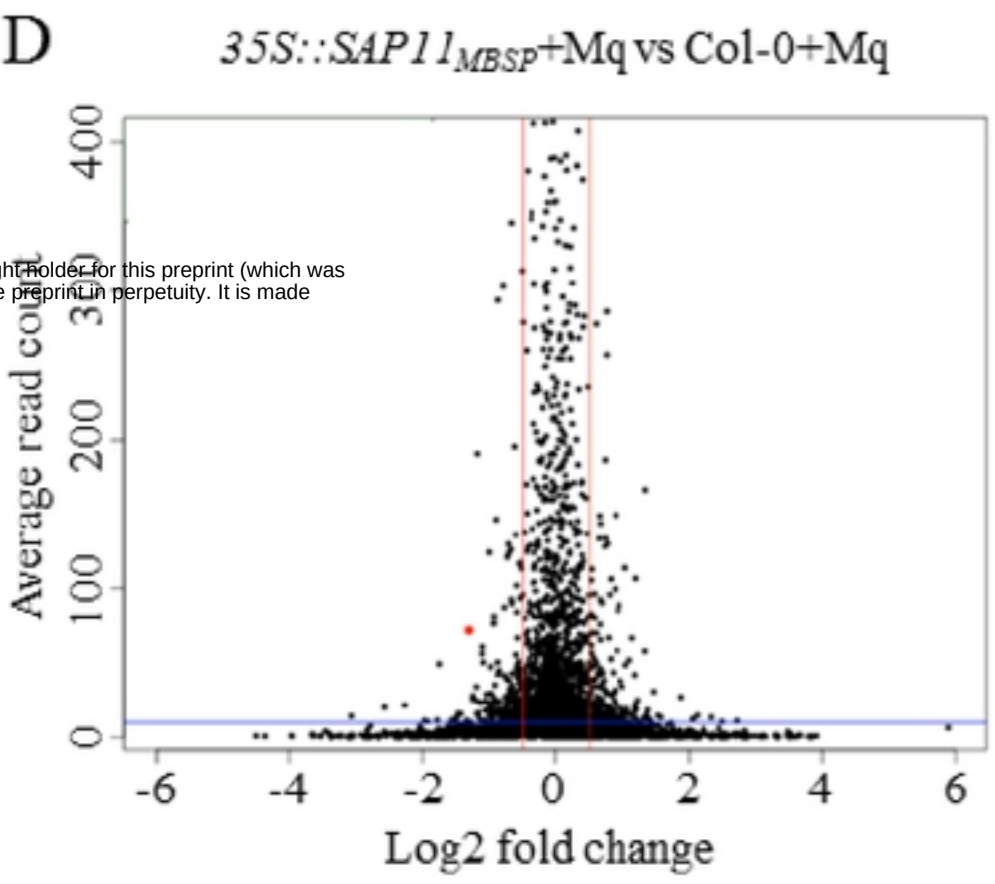

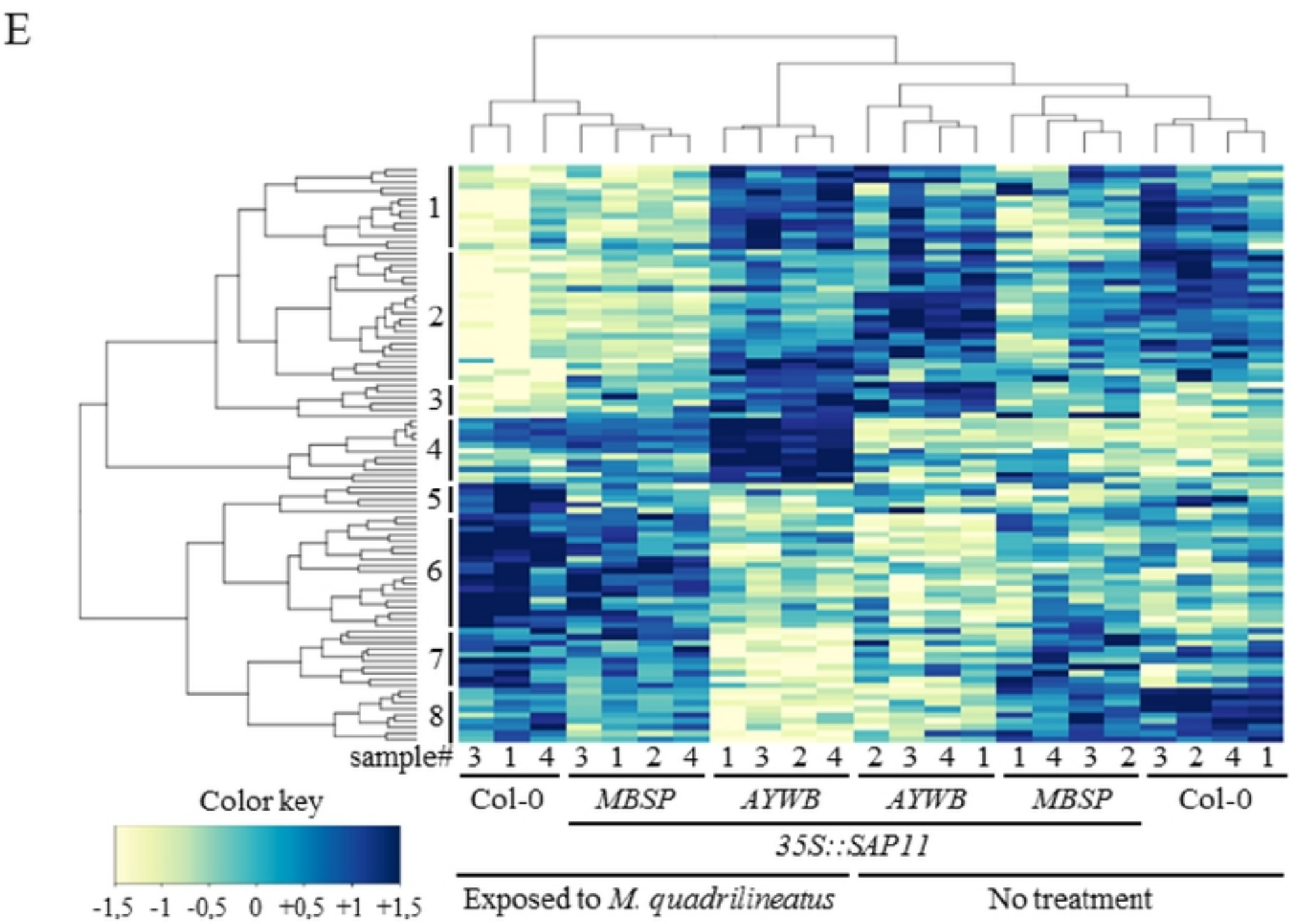

Fig3

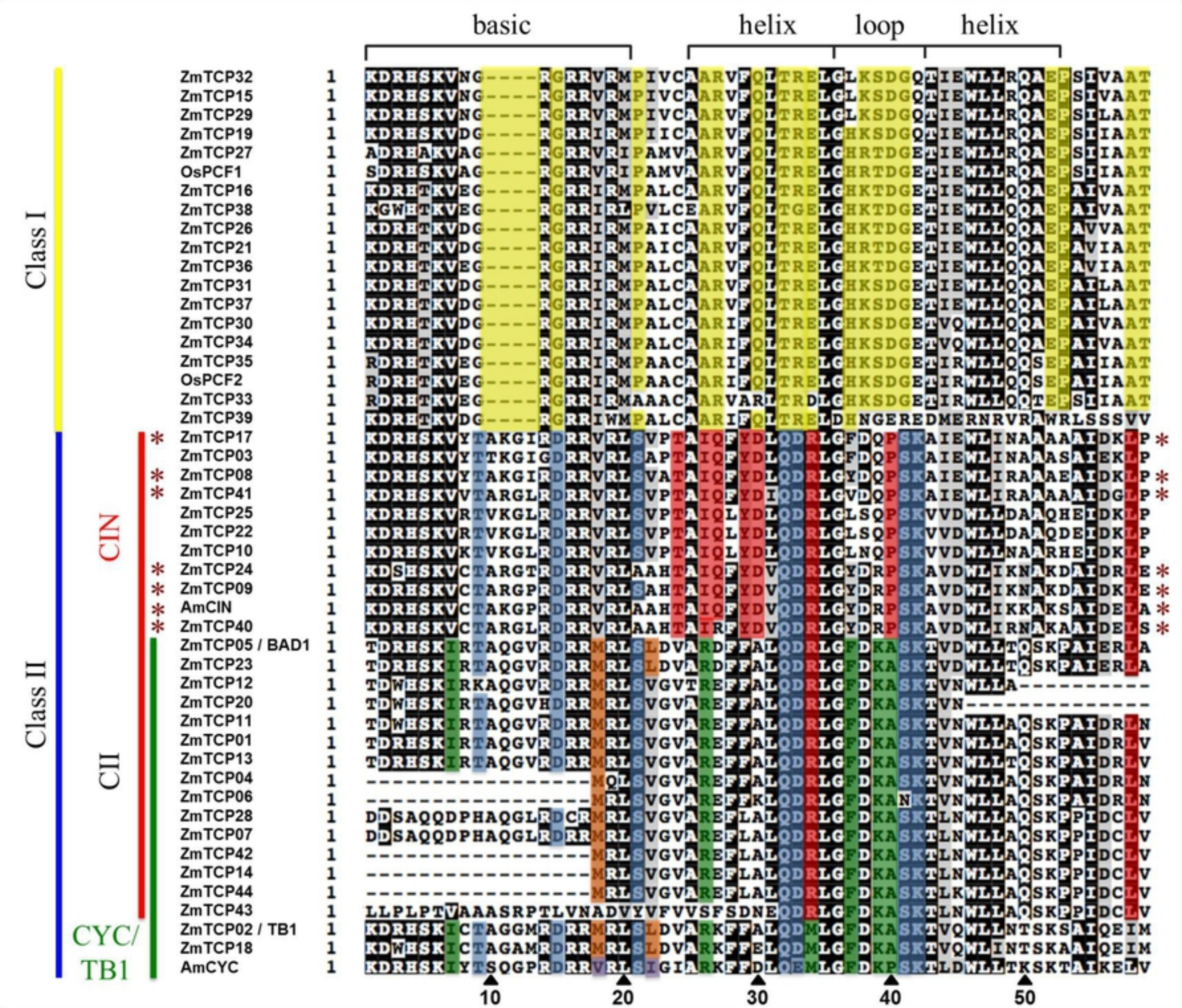
basic
helix
loop
helix
Class I
Class II
CIN
CII
CYC/
TB1
ZmTCP32
ZmTCP15
ZmTCP29
ZmTCP19
ZmTCP27
OsPCF1
ZmTCP16
ZmTCP38
ZmTCP26
ZmTCP21
ZmTCP36
ZmTCP31
ZmTCP37
ZmTCP30
ZmTCP34
ZmTCP35
OsPCF2
ZmTCP33
ZmTCP39
ZmTCP17
ZmTCP03
ZmTCP08
ZmTCP41
ZmTCP25
ZmTCP22
ZmTCP10
ZmTCP24
ZmTCP09
AmCIN
ZmTCP40
ZmTCP05 / BAD1
ZmTCP23
ZmTCP12
ZmTCP20
ZmTCP11
ZmTCP01
ZmTCP13
ZmTCP04
ZmTCP06
ZmTCP28
ZmTCP07
ZmTCP42
ZmTCP14
ZmTCP44
ZmTCP43
ZmTCP02 / TB1
ZmTCP18
AmCYC
10
20
30
40
50

Fig4

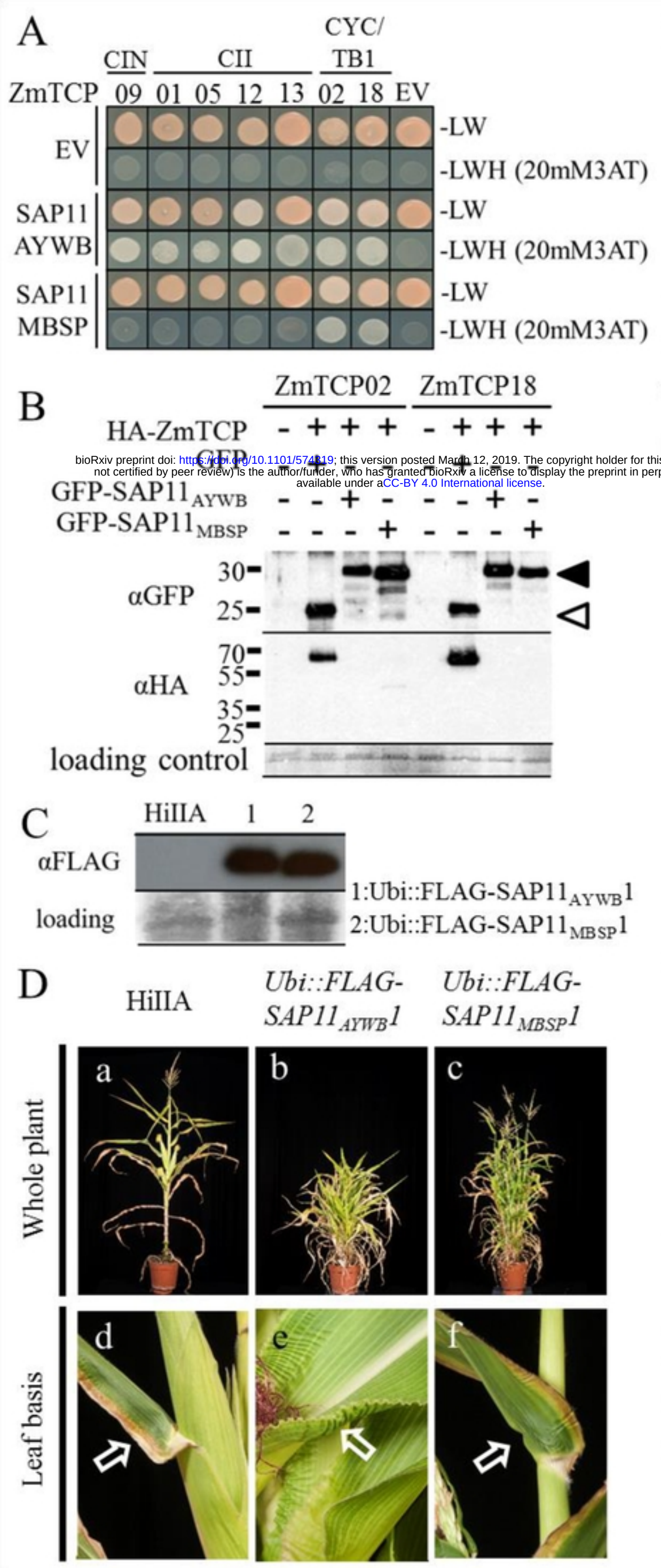

Fig5

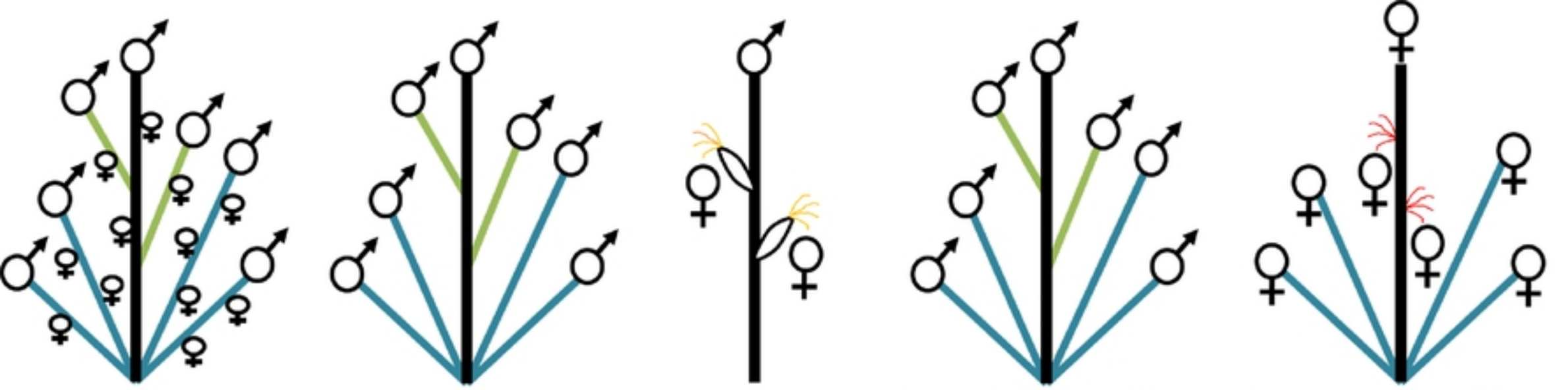

Teosinte
[39,47]

tb1 (*Z. mays*)
[39,46]

Z. mays
HiIIA

Ubi::FLAG-SAP11$_{MBSP}$
(HiIIA)

Ubi::FLAG-SAP11$_{AYWB}$
(HiIIA)

Fig6

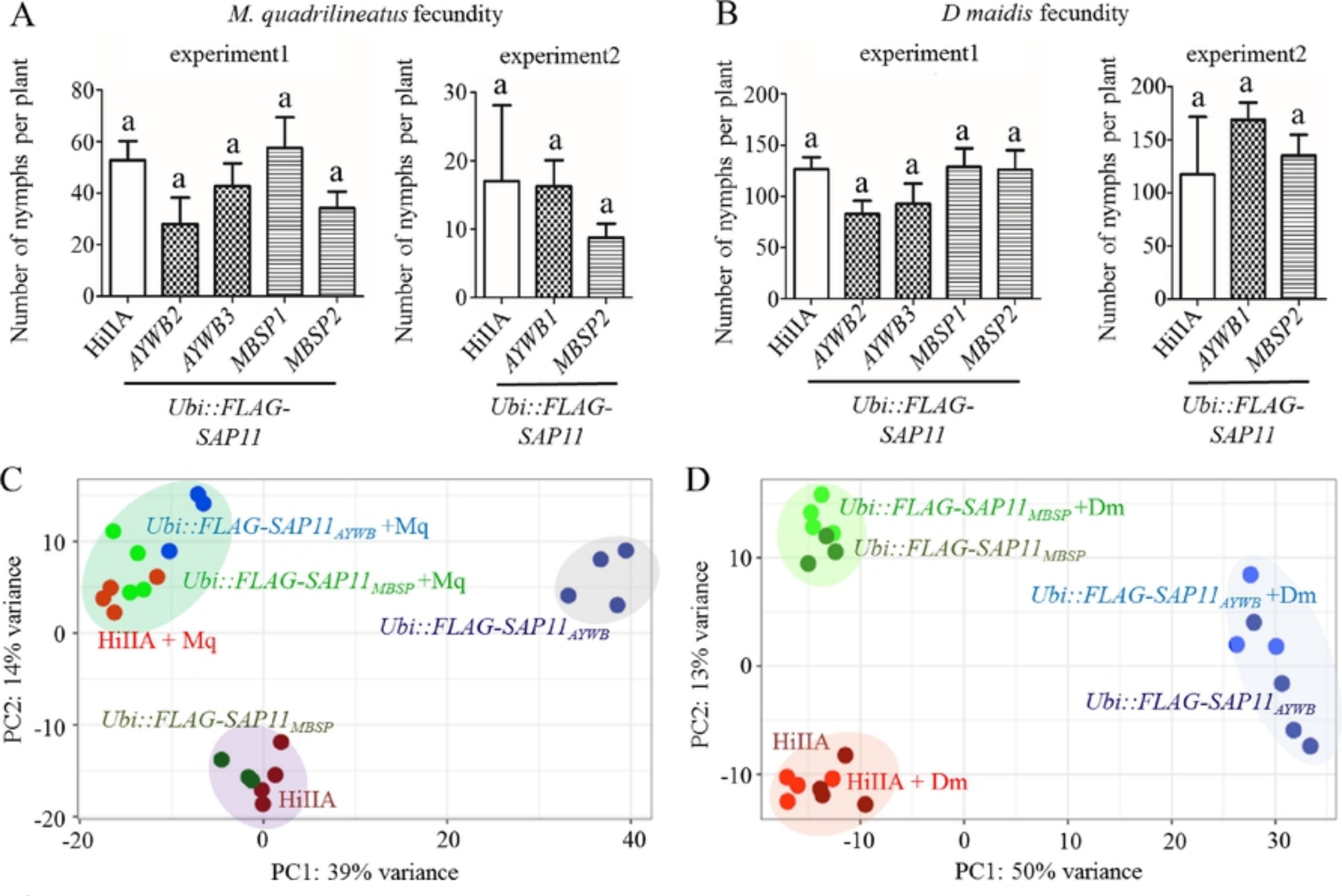
A
M. quadrilineatus fecundity
experiment1
Number of nymphs per plant
80
60
40
20
0
a
a
a
a
a
HiIIA
AYWB2
AYWB3
MBSP1
MBSP2
Ubi::FLAG-SAP11
experiment2
30
20
10
0
a
a
a
HiIIA
AYWB1
MBSP2
Ubi::FLAG-SAP11
B
D maidis fecundity
experiment1
200
150
100
50
0
HiIIA
AYWB2
AYWB3
MBSP1
MBSP2
Ubi::FLAG-SAP11
experiment2
HiIIA
AYWB1
MBSP2
Ubi::FLAG-SAP11
C
Ubi::FLAG-SAP11AYWB +Mq
Ubi::FLAG-SAP11MBSP +Mq
HiIIA + Mq
Ubi::FLAG-SAP11AYWB
Ubi::FLAG-SAP11MBSP
HiIIA
PC2: 14% variance
PC1: 39% variance
10
0
-10
-20
-20
0
20
40
D
Ubi::FLAG-SAP11MBSP +Dm
Ubi::FLAG-SAP11MBSP
Ubi::FLAG-SAP11AYWB +Dm
Ubi::FLAG-SAP11AYWB
HiIIA
HiIIA + Dm
PC2: 13% variance
PC1: 50% variance
10
0
-10
-10
0
10
20
30

Fig7